European Journal of Medicinal Chemistry 108 (2016) 701–719

Contents lists available at ScienceDirect

European Journal of Medicinal Chemistry

journal homepage: http://www.elsevier.com/locate/ejmech

Research paper

Synthesis, biological evaluation and molecular modeling of a novel series of 7-azaindole based tri-heterocyclic compounds as potent CDK2/Cyclin E inhibitors

Christine B. Baltus [a, 1], Radek Jorda [b, **, 1], Christophe Marot [a], Karel Berka [c, d], Václav Bazgier [b, d], Vladimír Kryštof [b], Gildas Prié [a], Marie-Claude Viaud-Massuard [a, *]

[a] UMR 7292 GICC Equipe 4 Innovation Moléculaire et Thérapeutique, Labex SYNORG, University of Tours, Faculty of Pharmacy, 31 Avenue Monge, 37200 Tours, France
[b] Laboratory of Growth Regulators & Department of Chemical Biology and Genetics, Centre of the Region Haná for Biotechnological and Agricultural Research, Palacký University and Institute of Experimental Botany AS CR, Šlechtitelů 27, CZ-78371 Olomouc, Czech Republic
[c] Regional Centre of Advanced Technologies and Materials, Department of Physical Chemistry, Faculty of Science, Palacky University Olomouc, 17. Listopadu 12, 77146 Olomouc, Czech Republic
[d] Department of Physical Chemistry, Faculty of Science, Palacký University, 17. Listopadu 1192/12, 771 46 Olomouc, Czech Republic

ARTICLE INFO

Article history:
Received 28 October 2015
Received in revised form
11 December 2015
Accepted 12 December 2015
Available online 19 December 2015

Keywords:
Cyclin-dependent kinase 2
Kinase inhibitors
Anti-tumor agent
1*H*-pyrrolo[2,3-*b*]pyridine
[3 + 2] cycloaddition
1,4-Triazole
1,5-Triazole
3D-QSAR CoMFA

ABSTRACT

From four molecules, inspired by the structural features of fascaplysin, with an interesting potential to inhibit cyclin-dependent kinases (CDKs), we designed a new series of tri-heterocyclic derivatives based on 1*H*-pyrrolo[2,3-*b*]pyridine (7-azaindole) and triazole heterocycles. Using a Huisgen type [3 + 2] cycloaddition as the convergent key step, 24 derivatives were synthesized and their biological activities were evaluated. Comparative molecular field analysis (CoMFA), based on three-dimensional quantitative structure–activity relationship (3D-QSAR) studies, was conducted on a series of 30 compounds from the literature with high to low known inhibitory activity towards CDK2/cyclin E and was validated by a test set of 5 compounds giving satisfactory predictive r^2 value of 0.92. Remarkably, it also gave a good prediction of pIC_{50} for our tri-heterocyclic series which reinforce the validation of this model for the pIC_{50} prediction of external set compounds. The most promising compound, **43**, showed a micro-molar range inhibitory activity against CDK2/cyclin E and also an antiproliferative and proapoptotic activity against a panel of cancer cell lines.

© 2015 Elsevier Masson SAS. All rights reserved.

1. Introduction

Cyclin-dependent protein kinases (CDKs) are universal eukaryotic cell cycle regulators that promote the passage through the restriction point, initiation of DNA replication, and mitosis [1]. Given the fact that CDKs have oncogenic potential and are amenable to pharmacological inhibition, their inhibitors have therefore attracted great interest as potential anticancer agents [2,3].

As a part of our research on medicinal chemistry, we are interested in developing new CDK inhibitors (CKIs), in particular towards CDK4/cyclin D and CDK2/cyclin E, since they both participate in the phosphorylation of the retinoblastoma protein (pRb). Each member of the pRb pathway (such as CDK4(6)/cyclin D, p16 and CDK2/cyclin E), which activates the transcription factors at the G1-S transition phase, which in its turn regulates the expression of several genes involved in DNA replication, can be deregulated in cancers. In some human cancers (such as lung cancer or leukemia), cyclin E (E1/E2) is over-expressed and CDK2 is hyper-activated [4]. Therefore, many CKIs have been developed and some of them are undergoing clinical trials [5]. Most inhibitors that entered clinical trials belong to the group of pan-selective CDK inhibitors [6], but some highly selective CDK inhibitors like THZ1 [7] or PD-0332991 [8] were also described (Fig. 1). However, simultaneous targeting of multiple CDKs (particularly CDK1 and 2) seems to be more

Abbreviation: CCR2, CC chemokine receptor 2; CCL2, CC chemokine ligand 2; CCR5, CC chemokine receptor 5.

* Corresponding author.
** Corresponding author.
E-mail addresses: radek.jorda@upol.cz (R. Jorda), marie-claude.viaud-massuard@univ-tours.fr (M.-C. Viaud-Massuard).

[1] These authors contributed equally.

http://dx.doi.org/10.1016/j.ejmech.2015.12.023
0223-5234/© 2015 Elsevier Masson SAS. All rights reserved.

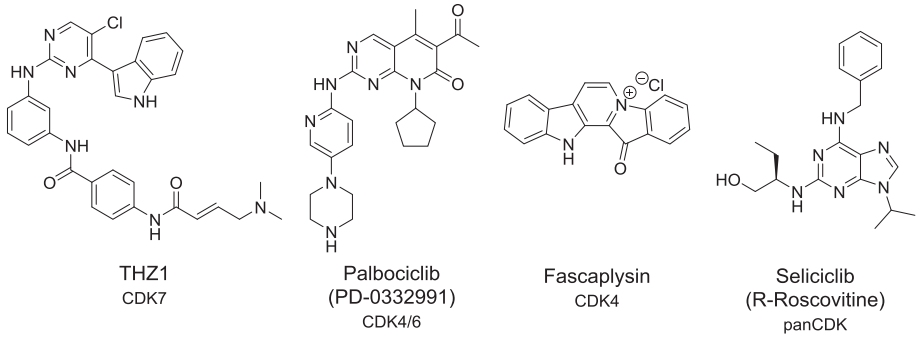

Fig. 1. Selected CDK inhibitors and their main CDK target.

advantageous in terms of anticancer activity, because many CDKs can compensate for the lack of others in cancer cells [9,10]. In addition, the knowledge about CDKs is growing constantly and it is still unclear whether observed effects are due to the activity of any single CDK or combinations of CDKs.

Since our laboratory has an expertise in the heterocyclic chemistry domain and by analogy with the structural features of a known CKI, fascaplysin [11] (IC_{50} CDK4/D = 0.35 μM) (Fig. 1), as other groups did with indole analogues [12–14], we designed and synthesized four novel heterocyclic molecules (**21**, **22**, **24** and **37**) (Figs. 2 and 3). **21** and **37** are composed of two 7-azaindole heterocycles linked each other by a 1,4- or 1,5-triazole type linker. The

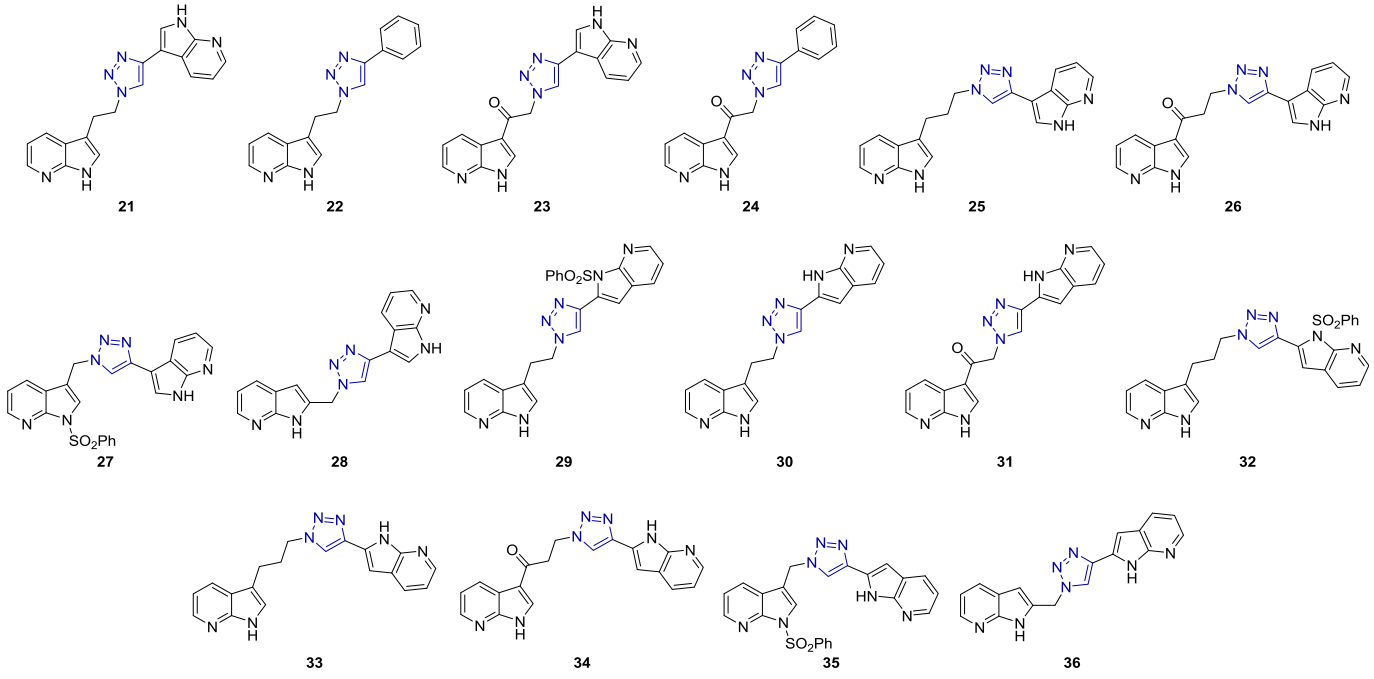

Fig. 2. 1,4-disubstituted triazole derivatives **21**–**36**.

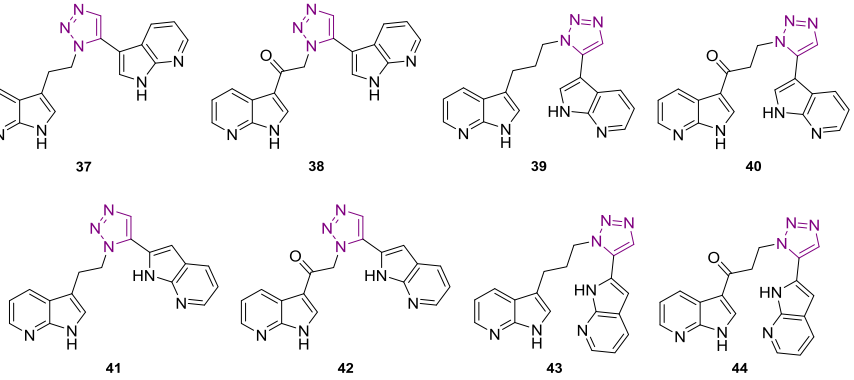

Fig. 3. 1,5-disubstituted triazoles derivatives **37**–**44**.

Table 1
Copper-catalyzed cycloaddition reaction.2

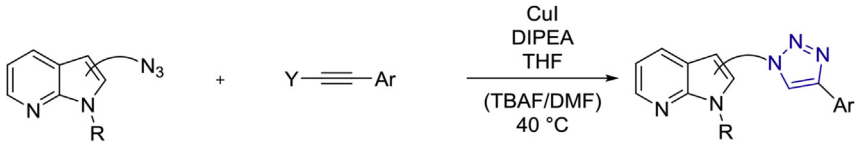

11, **12**, **16**, **20**
R = H, SO_2Ph

3a,**b**, **4a**,**b**: Ar = 7-azaindole;
Y = H, $SiMe_3$
4c: Ar = Ph ; Y = H

21-36

Entry	Azide	Alkyne	Additive[a]	Time (h)	Product	Yield (%)[b]
1	**11a**	**3a**	TBAF	24	**21**	83
2	**11a**	**4c**	–	16	**22**	80
3	**12a**	**3a**	TBAF	24	**23**	–
4	**12a**	**4c**	–	26	**24**	72
5	**12a**	**4a**	DMF	21	**23**	26
6	**11b**	**3a**	TBAF	20	**25**	38
7	**12b**	**3a**	TBAF	16	**26**	–
8	**12b**	**4a**	DMF	72	**26**	57
9	**16**	**4a**	–	16	**27**	68
10	**20**	**3a**	TBAF	18	**28**	59
11[c]	**11a**	**3b**	TBAF	18	**29 and 30**	43 and 39
12	**12a**	**4b**	DMF	16	**31**	84
13[c]	**11b**	**3b**	TBAF	16	**32 and 33**	47 and 37
14	**12b**	**4b**	DMF	16	**34**	57
15	**16**	**4b**	–	16	**35**	89
16	**20**	**3b**	TBAF	16	**36**	53

[a] TBAF 3 equivalents; DMF 1 mL.
[b] Isolated yields.
[c] Products obtained as a mixture and separated by chromatography on silica gel column [30].

third ring in **22** and **24** was replaced by a phenyl group. Their skeleton can be viewed as an open and non-planar structure of fascaplysin, where the indole ring was replaced by a 7-azaindole. This open form design gives a more flexible molecule which could allow a better fitting into the binding site of the enzyme. Moreover, contrary to fascaplysin, free rotation potential should avoid DNA intercalation [15].

The inhibitory activities of these four molecules were tested on recombinant CDK2/cyclin E and CDK4/cyclin D complexes. Although the results obtained for CDK4/cyclin D with **21** and **22** were not satisfactory [16], the inhibitory activities on CDK2/cyclin E of these four compounds were found to be interesting since the IC_{50} values of **21** and **37** are in the micro molar range (experimental pIC_{50}: 5.1, 4.0, 4.3 and 5.1 respectively for **21**, **22**, **24** and **37**) (Table 4).

In parallel, 3D-QSAR CoMFA analyses on known CDK2/cyclin E inhibitors were performed and the results allowed us to create and validate a model, which will be presented later in this article. Notably, the CDK2/cyclin E activity predictions obtained by this model for **21**, **22**, **24** and **37** were in good correlation with the experimental ones with a maximal difference of about 1 log (predicted pIC_{50}: 5.2, 5.3, 5.3 and 5.8 respectively for **21**, **22**, **24** and **37**)

Table 2
Ruthenium-catalyzed cycloaddition reaction.3

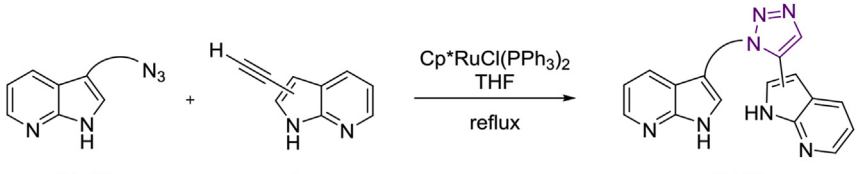

11, **12**

4

37-44

Entry	Azide	Alkyne	Time (h)	Product	Yield (%)[a]
1	**11a**	**4a**	60	**37**	41
2	**12a**	**4a**	20	**38**	90
3	**11b**	**4a**	20	**39**	73
4	**12b**	**4a**	20	**40**	18
5	**11a**	**4b**	20	**41**	62
6	**12a**	**4b**	20	**42**	97
7	**11b**	**4b**	20	**43**	18
8	**12b**	**4b**	20	**44**	34

[a] Isolated yields.

Table 3
Values of CoMFA models.

CoMFA	
Partial charge	Gasteiger–Huckel
q^2[a]	0.49
r^2[b]	0.99
S[c]	0.10
F value[d]	1021.002
N[e]	3
Contributions	
Steric	0.42
Electrostatic	0.58
Column filtering	2.0

[a] Cross-validated correlation coefficient.
[b] Non-cross-validated correlation coefficient.
[c] Standard error of estimate.
[d] F test value.
[e] Optimum number of components.

(Table 4).

Following these preliminary results, we decided to design a series of 7-azaindole based tri-heterocyclic derivatives to evaluate them towards CDK2/cyclin E, to predict their activity by our 3D-QSAR CoMFA model and validate the model by comparison with the experimental values, in order to develop new CDK2/cyclin E inhibitors as potential anti-cancer agents. The synthesis of these derivatives was based on the pharmacomodulation of **21** and **37**: i) attachment of the triazole linker chain on both sides at the C-2 or C-3 position of the 7-azaindole moiety, ii) variation of the linker chain length, iii) carbonyl function group kept or not on the linker chain, iv) 1,4- or 1,5-triazoles.

Herein is presented the synthesis of a new series of 7-azaindole based tri-heterocyclic molecules as potent CDK2/cyclin E inhibitors, a 3D-QSAR CoMFA model, and their biological evaluation.

2. Results and discussion

2.1. Chemistry

Tri-heterocyclic derivatives were synthesized via a key reaction, a Huisgen type [3 + 2] cycloaddition [17] between an alkyne and an azide function substituted on a 7-azaindole heterocycle. The alkyne function was introduced on the C-2 or the C-3 position of the 7-azaindole moiety via an halogenation reaction followed by a palladium-catalysed cross-coupling reaction (Sonogashira coupling reaction) [18–20] (Scheme 1).

In one hand, a simple iodation reaction on the commercially available 7-azaindole **1** led to the derivative **2** bearing the iodine atom on the C-3 position. The latter was treated with ethynyltrimethylsilane in a Sonogashira cross-coupling reaction catalyzed by $PdCl_2(PPh_3)_2$ and copper iodide in the presence of triethylamine. The alkyne **3a** could be used in the cycloaddition reaction either as prepared, or after the removal of the trimethylsilyl group in the presence of tetrabutylammonium fluoride (TBAF) as **4a** (Scheme 1).

In the other hand, the introduction of the iodine atom at the C-2 position is described in Scheme 1. A benzenesulfonyl group was introduced at the N-1 position of **1** using a classical procedure of amine protection with benzenesulfonyl chloride [21]. The protected derivative **5** was halogenated by iodine on the C-2 position, after deprotonation with a strong base, here lithium diisopropylamide (LDA) leading to the expected compound **6** (in a mixture with a diiodinated derivative, see exp. part, ^{1}H NMR ratio 1:0.34), result also observed by Naka et al. [22] (Scheme 1, pathway A). Due to the low yield obtained for **6**, we then decided to perform a two steps reaction at once, halogenation followed by deprotection of the amine function, yielding **7** in a good yield for the two steps (Scheme 1, pathway B). To introduce the desired alkyne function, the Sonogashira cross-coupling reaction was performed on **6** and **7** with ethynyltrimethylsilane. **3c** was obtained with a much better

Table 4
Antiproliferative, CDK2/E activity and CoMFA prediction data for studied compounds.

Cmpds	IC_{50} (μM)[a]	pIC_{50}	CoMFA prediction pIC_{50}	Cytotoxic activity in cancer cell lines IC_{50} (μM)[a]			Activation of caspases (fold)[b]
	CDK2/E			K562	MCF-7	G361	
21	7.2	5.1	5.2	39.5	87.1	44.2	1.2
22	>50	4.0	5.3	>50	>50	33.6	3.1
23	29.3	4.5	6.4	>25	>25	>50	2.2
24	>50	4.0	5.3	>25	>25	>50	1.5
25	6.1	5.2	6.1	66.6	60.7	36.9	3.9
26	17.8	4.7	5.4	44.27	64.7	>50	4.5
27	25.8	4.6	5.9	>25	>25	>50	7.5
28	18.4	4.7	5.0	>50	47.4	>50	2.1
29	>25	4.6	6.8	>25	>25	>50	2.1
30	30.0	4.5	4.7	>50	58.5	>50	4.5
31	9.2	5.0	5.4	>25	>25	>50	1.7
32	18.0	4.7	5.7	>25	>25	>50	1.8
33	8.7	5.1	4.2	>25	>25	>50	1.9
34	3.6	5.4	4.7	>25	>25	>50	1.2
35	>25	4.6	6.1	>25	>25	>50	1.6
36	1.9	5.7	5.9	>25	>25	>50	1.9
37	9.1	5.0	5.8	>25	>25	>50	1.9
38	1.1	6.0	6.4	>25	>25	>50	2.9
39	2.7	5.6	6.0	>25	>25	33.4	4.2
40	13.4	4.9	6.2	>25	>25	>50	3.3
41	27.6	4.6	5.5	>25	>25	>50	2.0
42	3.0	5.5	5.8	>25	>25	>50	2.2
43	2.0	5.7	5.6	39.9	>25	31.5	13.8
44	36.1	4.5	5.8	>25	>25	>50	n.d.
Roscovitine	0.2	–	–	30.9	27.2	20.8	n.d.
Imatinib	>100	–	–	0.73	>10	n.d.	n.d.

[a] Average values from at least three determinations.
[b] Relative caspase-3/7 activity in G361 melanoma cells after treatment with studied compounds at 50 μM concentration. Synthetic peptide Ac-DEVD-AMC was used as a substrate and caspase-3/7 activity was measured after 6 h by microplate reader at 346 nm/442 nm (excitation/emission).

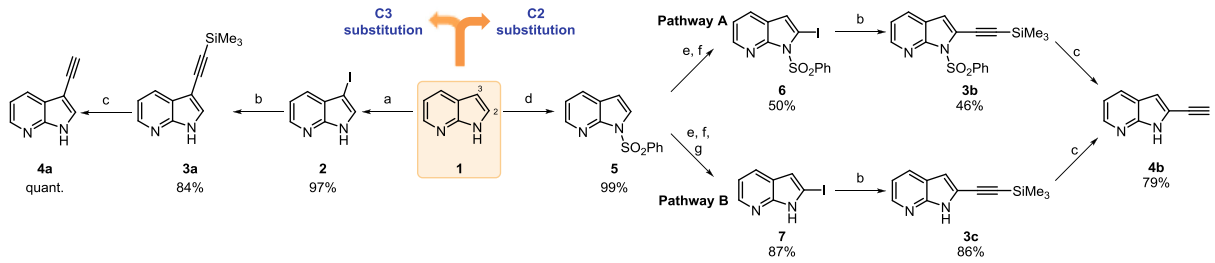

Reagents and conditions: a) I_2, KI, NaOH (1 M), EtOH, RT, 16 h. b) Ethynyltrimethylsilane, $PdCl_2(PPh_3)_2$, CuI, Et_3N, THF, RT, 20 h. c) TBAF, THF, RT, 2 h. d) Benzenesulfonyl chloride, TBAB, NaOH, CH_2Cl_2, 0 °C, RT, 1 h. e) LDA, THF, - 60 °C, 30 min. f) I_2, - 60 °C to RT, 16 h. g) NaO*t*Bu, dioxane, reflux, 1 h.

Scheme 1. Synthesis of the alkyne derivatives **3** and **4**.

yield than **3b** (86% and 46% respectively). The trimethylsilyl group of **3c** was removed with TBAF [23] leading to the derivative **4b**. The removal of the trimethylsilyl group in **3b** was attempted without success, as the reaction conditions led to the removal of both trimethylsilyl and benzenesulfonyl protecting groups, ending up to the unprotected derivative **4b** in 79% yield. The pathway B was found to be the pathway of choice for the synthesis of **4b** since it gave a better overall yield compared to pathway A, 59% and 18% respectively.

In parallel, different length carbon chains bearing the desired azide function were introduced at the C-3 and C-2 (Scheme 2) positions of the 7-azaindole heterocycle.

First, concerning the compounds substituted at the C-3 position, **1** was reacted in a Friedel and Craft acylation reaction with selected acid chlorides (**8a** and **8b**) yielded the derivatives **9a** and **9b** containing a 2 or 3 carbons chain. The carbonyl group in **9** could be kept

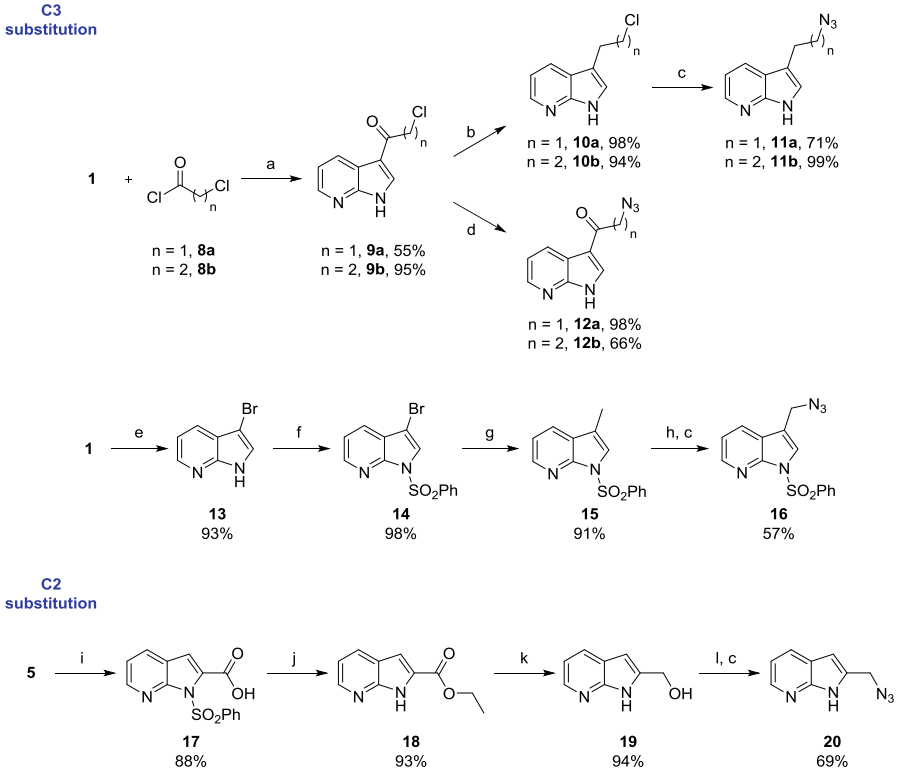

Reagents and conditions: a) $AlCl_3$, CH_2Cl_2, RT, 16 h. b) $LiAlH_4$, $AlCl_3$, DME, 0 °C, then RT, 16 h. c) NaN_3, DMF, H_2O, 60 °C, 16 h. d) NaN_3, DMF, H_2O, 60 °C, 16 h or RT, 36 h. e) NBS, CH_2Cl_2, 0 °C, RT, 16 h. f) Benzenesulfonyl chloride, TBAB, NaOH, CH_2Cl_2, 0 °C, RT, 1 h. g) $AlMe_3$, $Pd(PPh_3)_4$, THF, 60 °C, 24 h. h) NBS, AIBN, CCl_4, reflux, 16 h. i) LDA, THF, -35 °C, then CO_2, -55 °C, RT, 16 h; HCl. j) EtOH, H_2SO_4, reflux, 20 h. k) $LiAlH_4$, DME, RT, 16 h. l) $SOCl_2$, CH_2Cl_2, RT, 1 h.

Scheme 2. Synthesis of the azide derivatives.

or reduced with lithium aluminium hydride ($LiAlH_4$) in the presence of aluminium chloride ($AlCl_3$) [24] (leading to **10**) before the substitution of the chlorine atome by the azide group with sodium azide was set up. The azide derivatives **11** and **12** were obtained in moderate to good yields (Scheme 2).

The 7-azaindole derivative **16**, substituted in C-3 by a methylene azide group, was obtained in a 4 steps synthetic procedure from **1** (Scheme 2). Bromination of **1** at the C-3 position by *N*-bromosuccinimide (NBS) yielded **13**, which was protected with a benzenesulfonyl group. The derivative **14** was methylated at the C-3 position with $AlMe_3$ using tetrakis(triphenylphosphine)palladium as catalyst [25,26] to afford **15** in a good yield. Bromination of the methyl group with NBS and azobisisobutyronitrile (AIBN) [27] followed by a nucleophilic substitution with sodium azide led to **16** in moderate yield for the two steps.

Alternatively, the methylene azide scaffold was introduced on the C-2 position of the heterocycle (Scheme 2). The acid derivative **17** was obtained by deprotonation of **5** by LDA followed by the addition of carbon dioxide. The compound **17** was esterified with ethanol yielding **18**, which was reduced to the alcohol **19** by using $LiAlH_4$ in dimethoxyethane (DME). The hydroxyl group newly formed was substituted by a chlorine, in the presence of thionyl chloride, which was itself substituted by the azide group leading to the derivative **20** in good yield.

The alkyne (**3** and **4**) and azide (**11**, **12**, **16** and **20**) derivatives were then engaged in [3 + 2] cycloaddition reactions. Depending on the chosen catalyst, copper or ruthenium, the reaction led to 1,4- or 1,5-disubstituted triazole respectively.

First, copper (I) iodide was used as catalyst for the copper-catalyzed [3 + 2] Huisgen cycloaddition reaction in the presence of diisopropylethylamine (DIPEA) in THF (Table 1) [28]. An attempt using copper sulfate and sodium ascorbate was made but it did not give as good results as with copper iodide (results not shown). The corresponding 1,4-disubstituted triazoles **21**–**36** (Fig. 2) were obtained with moderate to good yields in 16 h–72 h. When the non-terminal alkyne derivatives **3a** and **3b** were used as starting materials, this reaction was carried out in a one pot procedure together with the deprotection of the trimethylsilyl group by TBAF (Table 1, entries 1, 3, 6, 7, 10, 11, 13 and 16) [29]. However, when this one pot reaction was tested on the azide derivatives containing a carbonyl function **12**, the reaction did not occur (Table 1, entries 3 and 7). In this case, terminal alkyne derivatives (**4a**, **4b** or phenylacetylene **4c**) had to be used in order to obtain the expected tri-heterocycle derivatives (Table 1, entries 4, 5, 8, 12 and 14). Moreover, due to the poor solubility of **12a** and **12b** in THF, small amount of dimethylformamide (DMF) was added in the reaction mixture. This copper-catalyzed reaction led to the obtention of a series of 1,4-disubstituted triazole derivatives shown in Fig. 2.

Secondly, terminal alkyne (**4**) and azide (**10** and **12**) derivatives were engaged in a ruthenium-catalyzed [3 + 2] cycloaddition reaction with pentamethylcyclopentadienylbis(triphenylphosphine) ruthenium(II) chloride ($Cp^*RuCl(PPh_3)_2$) in THF (Table 2) [31]. The 1,5-disubstituted triazole derivatives (**37**–**44**), obtained in low to good yields in 20 h–60 h, are presented in Fig. 3.

To conclude, all 24 synthesized compounds have consisted of three parts: 7-azaindole, triazole and aryl part. The first heterocycle, 7-azaindole, is linked by carbon C2 or C3 to nitrogen N1 of triazole in all derivatives, third aryl is linked to triazole at position 4 or 5 resulting two series: 1,4-disubstituted (**21**–**36**) and 1,5-disubstituted triazoles (**37**–**44**). Both series are subdivided to two another libraries differing by binding of third aryl (mainly 7-azaindole) to triazole. While compounds **29**–**36** and **41**–**44** bind by carbon C2 of 7-azaindole to triazole, the rest of compounds containing 7-azaindole (**21, 23, 25**–**28, 37**–**40**) bind through carbon C3 to triazole. Only two derivatives (**22**, **24**) have varied from the whole series by presence of phenyl group instead of 7-azaindole ring.

2.2. 3D-QSAR model

To rationalize the design and, thus, to understand physiochemical properties and structural parameters of the pharmacophore, a three-dimensional quantitative structure activity relationship (3D-QSAR) study of numerous CKIs derivatives by comparative molecular field analysis (CoMFA) [32] was performed. Traditional QSAR models are unable to explain complex structure activity data because of the extreme specificity of biological activity described by 3D intermolecular forces and predicted on 3D molecular structures. Consequently, the most relevant QSAR model would be shape-dependent and would describe steric and electrostatic interactions with sufficient accuracy. Indeed, the comparative molecular field analysis (CoMFA) method meets these requirements and has become a powerful tool for studying 3D-QSAR.

A CoMFA study starts by the examination of the differences in targeted properties which are related to changes in the shape of the steric and electrostatic fields surrounding the molecules. A QSAR table is then used to accommodate the details of the shape of each field by sampling their magnitudes at regular intervals throughout a specified region of space [32]. Similarity indices are calculated at regularly spaced grid points for the prealigned molecules. Instead of the direct measurement of the similarity between all mutual pairs of a molecule, indirect evaluation of the similarity of each molecule in the data set with a common probe atom is calculated [33]. A linear regression equation of similarity with biological activities is finally derived.

This indirect ligand-based approach can assist in understanding structure–activity relationships (SARs) and can also serve as a tool in designing more potent anticancer agents. We believe this study provides useful information about the structural requirements of CDK2 inhibitors, and expect the results will aid in the design of new synthetic drugs.

2.3. Computational methods

2.3.1. Data sets

A total of 30 ligands from the literature, 25 for the training set (**L1**-**L25**) and 5 for the test set (**L26**-**L30**), with known structures and biological activities towards CDK2/cyclin E, were used in the study (See Supp. Info. Tables S1 and S2) [34]. The IC_{50} values were converted to the corresponding pIC_{50} ($-\log IC_{50}$) and used as dependent variables in CoMFA analyses. The pIC_{50} values span a range of 4.5 log units, providing a broad and homogenous data set for the 3D-QSAR study. The initial structures of 30 compounds were constructed using the Scketch Builder module on Sybyl X 2.1 (TRIPOS) [35]. Conformations of compounds in the training set and test set were generated using the multisearch utility in Sybyl X 2.1. The conformer with the lowest energy was extracted and energy minimization was performed using the Tripos force field [36], with a distance-dependent dielectric constant, and the Powell conjugate gradient algorithm, with a convergence criterion of 0.01 kcal mol^{-1}.

2.3.2. Molecular alignment

Structural alignment is one of the most sensitive parameters in 3D-QSAR analyses. The accuracy of the prediction of CoMFA models and the reliability of the contour models depend strongly on the structural alignment of the molecules [37]. The molecular alignment of the training set was achieved by the Sybyl X 2.1 routine docking (FlexX) with X-ray crystal structure of CDK2 (PDB: 2A4L) (Fig. 4a). In order to investigate the interaction mechanism

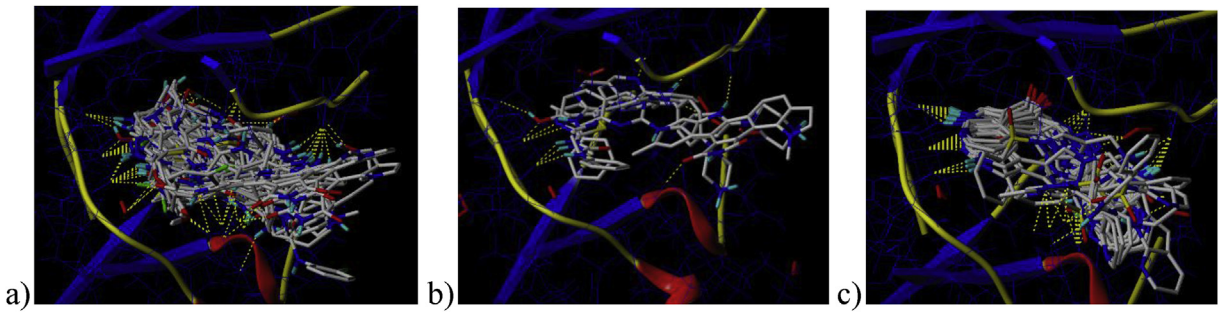

Fig. 4. Alignment in the active site of CDK2 (PDB: 2A4L) of a) training set ligands **L1**-**L25**, b) test set ligands **L26**-**L30**, c) our designed ligands **21**–**44**.

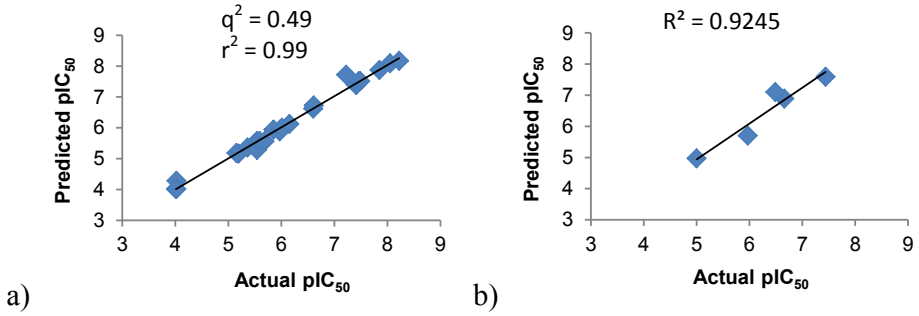

Fig. 5. CoMFA predicted and actual activities of ligands from a) the training set, b) the test sets.

between the ligand and the targeted enzyme, the molecular docking analysis was performed based on the active site of the built 3D model of 2A4L. The FlexX docking methods [38] were used to explore the reasonable binding mode of ligands in the active site of 2A4L. Once the molecules from the training set are docked, the poses with the best docking score values were selected as the aligned molecules used for the CoMFA study.

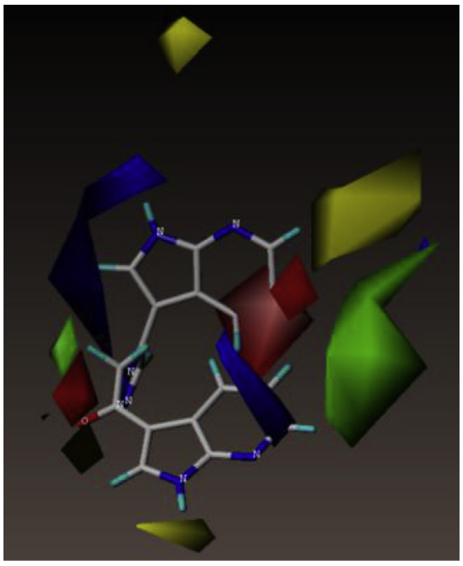

Fig. 6. Contour plot using CoMFA steric and electrostatic fields for CDK2 inhibitors with **38**. Green indicates regions where bulky groups increase activity; yellow indicates regions where bulky groups decrease activity; blue indicates regions where positive charges increase activity or negative charges decrease it; red indicates regions where negative charges increase activity or positive charges decrease it. (For interpretation of the references to color in this figure legend, the reader is referred to the web version of this article.)

2.3.3. CoMFA studies

Sybyl X 2.1 was used for molecular modeling and 3D-QSAR analysis on a PC workstation equipped with an Intel(R) Xeon(R) CPU 2.67 GHz processor. Steric and electrostatic CoMFA fields were calculated using the Lennard-Jones and the Coulomb potentials.[32] The partial atomic charge was calculated by the Gasteiger-Hückel method [39]. Default parameters (Tripos force field, dielectric distance $1/r^2$, steric and electrostatic cut-off 30 kcal mol^{-1}, positively charged sp^3 hybridized carbon atom, grid spacing 2 Å) were used unless stated otherwise. With standard options for scaling of variables, the regression analysis was carried out using the full cross-validated partial least squares (PLS) method (leave one out) [40]. To derive 3D-QSAR models, the CoMFA descriptors were used as independent variables and the pIC_{50} as the dependent variable. Partial least squares (PLS) regression analysis was conducted with the standard implementation in the Sybyl X 2.1 package. The predicted values of the models were evaluated by leave-one-out cross-validation [41] (Table 3).

2.3.4. Predictive power of CoMFA models

To test the predictability of the analyses, the activities of training set compounds were calculated from the best CoMFA model considering Gasteiger-Hückel partial charges, steric and electrostatic field combinations. The correlation between experimental and predicted training set activities is shown in Fig. 5a and indicates a good agreement between experimental and predicted values (See Supp. Info. Table S1).

A test set made of 5 compounds was used to verify the efficacy of the CoMFA model (See Supp. Info. Table S2). These 5 molecules were aligned in the active site of the enzyme in the same way as the training set (Fig. 4b). Fig. 5b shows that the test set pIC_{50} predictions and the actual pIC_{50} were in a similar range of values (See Supp. Info. Table S2), giving a predictive correlation coefficient r^2 of

0.92, which validates this model.

Once the model was validated with the test set, our 24 tri-heterocyclic derivatives were aligned in the active site of the enzyme (Fig. 4c) and the CoMFA allowed us to obtain a prediction for their inhibitory activities (pIC_{50}) (Table 4).

2.3.5. CoMFA contour maps

The CoMFA steric and electrostatic fields from the final non-cross-validated analysis were plotted as 3D colored contour maps. In these contour maps, each colored contour represents particular properties (Fig. 6): green for regions of high steric tolerance (80% contribution), yellow for low steric tolerance (20% contribution), red for regions of decreased tolerance for positive charge (20% contribution) and, blue for regions of decreased tolerance for negative charge (80% contribution). The larger size of the green–yellow region compared to the red–blue region indicates a greater contribution of steric fields than electrostatic ones in determining the biological activity. The derivative **38** was selected to feature in the CoMFA contour map (Fig. 6), since it was the tri-heterocyclic derivative having the best IC_{50} value on the recombinant CDK2/cyclin E complex (Table 4). Indeed, the carbonyl group in **38** was located in a region of negatively charged electrostatic field and the whole molecule seemed to meet the requirement of the steric constraints.

In this study, 3D-CoMFA QSAR analyses were used to predict the CDK2/cyclin E inhibitory activity of a set of tri-heterocyclic compounds. The QSAR model gave good statistical results in terms of q^2 and r^2 values, respectively 0.495 and 0.99. The CoMFA model provided the most significant correlation of steric and electrostatic fields with the biological activities. Overall, the CoMFA method provided a better statistical model, which implies the significance of steric and electrostatic fields in the selectivity and activity of these compounds. The statistical significance and robustness of the 3D-QSAR models generated were confirmed using a test set ($r^2 = 0.92$). The effects of the steric, electrostatic fields around the aligned molecules on their activities were clarified by analyzing the CoMFA contour maps. Most of our compounds (~70%) were predicted with a maximum deviation of 1 log unit. The micromolar range activity of our best compounds were correctly predicted (**36**, **38**, **39**, **42** and **43**), since the predictive deviation is only about 0.5 log unit. Only a few inactive compounds were predicted with a micromolar activity (however, this shows that our model do not miss potent compounds).

2.4. CDK inhibition

The 24 tri-heterocyclic derivatives synthesized were tested for CDK2/cyclin E kinase inhibition. The obtained data are presented in Table 4.

The majority of these compounds displayed submicromolar activities toward CDK2, what we consider as a good starting point for further improvement of molecules. The structural diversity of library allowed us to evaluate structure–activity relationships. The first observed trend is related to substitution of 7-azaindole at nitrogen N1 by bulky phenylsulphonyl moiety that leads to a decrease of CDK2 activity of unmodified molecules (compared pairs **27**–**28, 29**–**30, 32**–**33, 35**–**36**). No measurable CDK inhibition of two compounds bearing phenyl group as a third aryl (compounds **22, 24**) showed us that 7-azaindole as a third heterocycle is beneficial (probably due to the presence of nitrogen N1 as a hydrogen donor). In fact, CDK2 inhibition was also reduced mostly with the shortening of the alkyl chain between first 7-azaindole and triazole (compared pairs **30**–**33**, **37**–**39, 41**–**43**). In addition, modification of alkyl chain can also influence the activity; while the presence of a keto group leads to increase of CDK2 inhibitory activity in comparison with unmodified structures (pairs **30**–**31, 33**–**34, 37**–**38, 41**–**42**), in some pairs the activity decreased (pairs **21**–**23, 25**–**26, 39**–**40, 43**–**44**). Observed differences are probably related to the orientation of the whole molecules in the active site of kinase and with the possibility to use the carbonyl as a hydrogen bond acceptor. The most active compounds from this library belong to the group of 1,5-disubstituted triazoles (structural isomers **38**–**42, 39**–**43**) and their IC_{50}(CDK2) reaches 1.1 μM (Table 4).

2.5. Flexible docking

To further explore SAR of novel compounds we decided to use our flexible docking procedure in conjunction with the Autodock Vina molecular docking program to model binding interactions with CDK2 (see the Experimental section for details). Crystal structure (PDBID: 2A4L) reveals that the ATP binding groove is formed by a planar, mainly hydrophobic, pocket between Ile10 and Leu134. On the edge of this pocket are situated main chains of Glu81 and Leu83 forming hydrogen bond acceptor-donor-acceptor pattern for interaction with purine bases of roscovitine or ATP. The pocket further tilts and extends towards the bay between two polar residues His84 and Lys89. This bay is filled with phenyl moiety of roscovitine in the crystal structure, but it can also accommodate larger ligands, such as biaryls [42].

Our molecular docking showed the binding mode of molecule **43** within the binding pocket of CDK2 kinase (Fig. 7; binding energy −9.5 kcal/mol). The ligand forms a U-shape with two branches formed by 7-azaindoles and turning loop formed by triazole moiety. Triazole shows two interactions – directly with Thr14 and more distantly with Asp145 (possibly through water molecule). First 7-azaindole branch interacts with the typical main chain interactions – Glu81 and Leu83. Second branch seems to be more movable as it has just intraction with main chain of Glu12, whereas it is more exposed to the water.

2.6. Anticancer activity in vitro

Table 4 and Table S4 (See Supp. Inf.) summarized also anticancer activity of prepared compounds towards three cancer cell lines.

Inhibition of CDKs in cells either by chemical or genetic depletion lead to the i) reduction of cell proliferation, ii) changes in cell cycle profile and iii) induction of apoptosis [43,44].

We therefore analyzed the antiproliferative and proapoptotic activity of all derivatives to confirm reported inhibition of CDKs. First, we treated a panel of cancer cell lines with increasing concentrations and determined the compounds cytotoxicity (IC_{50}) after 72 h (Table 4). Unexpectedly, majority of compounds did not display measurable IC_{50}, due to the limited solubility in culture medium. Otherwise, we determined the IC_{50} values of the most active derivatives reaching up to mid-micromolar ranges (Table 4).

The most active compound **43** was further profiled on a additional cancer cell lines (See Supp. Info. Table S3).

In parallel, we tested the ability of our compounds to activate apoptosis in treated G361 cells after 24 h at a single dose of 50 μM. Using the one-step cellular caspase-3/7 activity assay [45] we determined that many compounds increased caspases activity over untreated control cells (Table 4); compound **43** more than ten-times and therefore we chose **43** as a candidate and evaluated its biological effects on melanoma G361 cell line in more detail.

In addition, the selectivity profile of the compound **43** was further characterized by assays on additional CDKs, including CDK1, CDK4, CDK5, CDK7 and CDK9. The compound yielded IC_{50} values in a mid-micromolar range (Table 5) and clearly showed that **43** is a pan-specific inhibitor of CDKs.

Asynchronously growing cells were treated by increasing

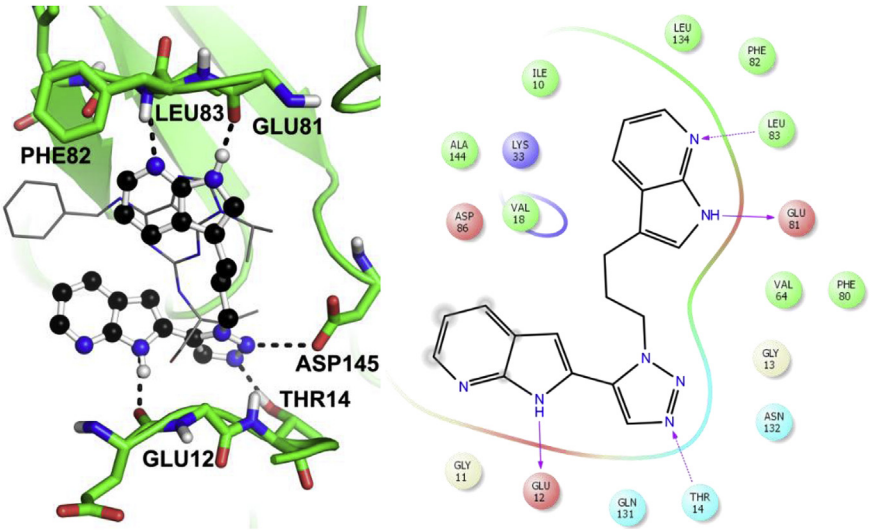

Fig. 7. Molecular docking of **43** into CDK2 (PDBID: 2A4L). Docking pose of **43** is shown on the left with ball and stick representation with annotated hydrogen bonds and roscovitine moiety in line representation. 2D interaction pattern of **43** is shown on the right. Amino acids within 3.5 Å from the ligand are shown whereas direct hydrogen bonds are shown with arrows. Solvent exposed part of the ligand is shown with circles.

Table 5
CDK selectivity profile for compound **43** and some known CDK inhibitors assayed as a control.

Kinases	IC_{50} (μM)[a]				
	43	Dinaciclib	BS-181	LY2835219	LDC000067
CDK1	11.5	0.072	14.0	0.371	3.95
CDK2	2.0	0.002	1.8	0.347	2.33
CDK4	9.0	0.127	44.7	0.005	3.16
CDK5	10.7	0.045	3.7	0.405	4.96
CDK7	>50	0.170	0.134	3.112	>20
CDK9	9.0	0.178	1.790	0.101	0.23

[a] Average values from at least three determinations.

concentrations of **43** for 24 h and then analyzed by flow cytometry. Compound **43** potently reduced population of actively-replicating cells (BrdU positive) in G361 (Fig. 8A) and MCF-7 (data not shown) cells and accumulated cells in G1 and G2/M phases. We also observed a dose-dependent increase in sub G1/apoptotic cells that reached up 34% for **43** (80 μM).

The previous analysis was complemented by the monitoring of the cellular expression of some cell cycle regulators in G361 cells treated with **43** for 24 h. We observed a rapid dose-dependent decrease of Rb level starting already after of 20 μM treatment. This inhibitory pattern corresponds to reduction of number of cells in S and G2/M phases upon treatment documented by decrease of protein levels of cyclins A and B (Fig. 8B).

In addition, we evaluated the effect of **43** on the

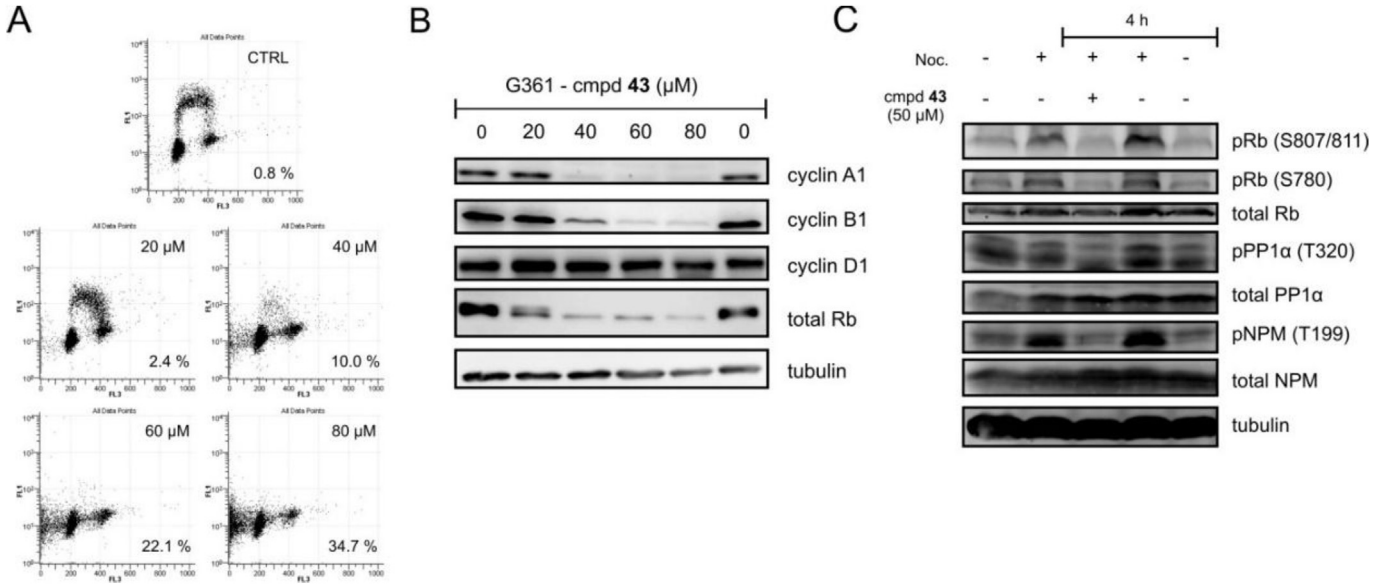

Fig. 8. A) Effect of compound **43** on cell cycle in G361 cells treated for 24 h. Flow cytometric analysis (10 000 counts) of DNA stained by propidium iodide (FL3 signal) and 5-bromo-2′-deoxyuridine (FL1 signal). The number in the lower right corner refers to the percentage of apoptotic cells (subG1 population). B) Immunobloting analysis of cell cycle-related proteins in G361 cells treated by compound **43** for 24 h. C) Compound **43** inhibits the phosphorylation of CDKs substrates. G361 cells were first synchronized with nocodazole (3 ng/mL for 16 h) and then treated with **43** as indicated. Substrates of CDKs were detected by immunoblotting analysis and tubulin was included as a control for equal protein loading.

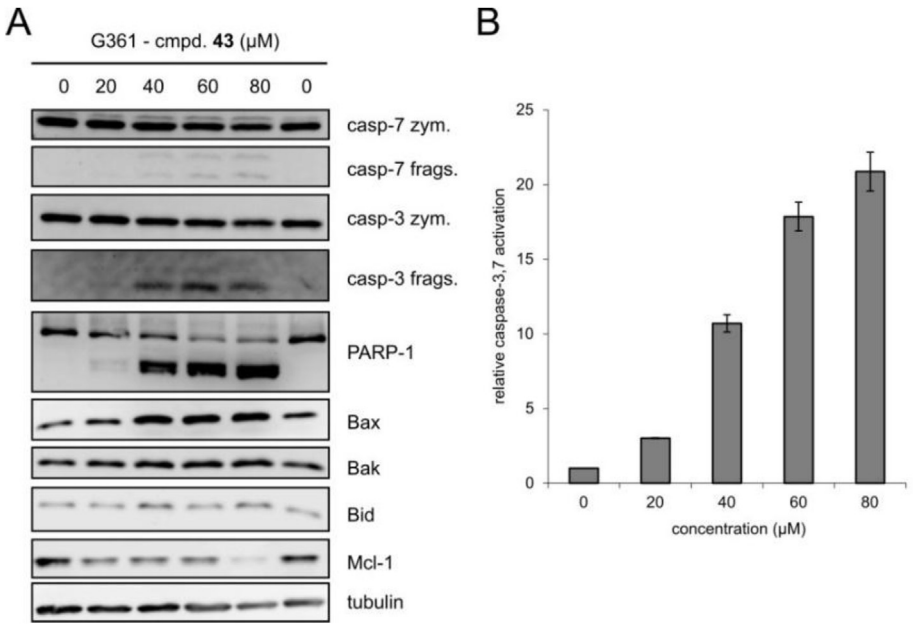

Fig. 9. A) Immunoblotting analysis of apoptosis-related proteins in G361 cells treated by compound **43** for 24 h. Tubulin level is included as a control for equal loading. B) Fluorimetric caspase-3,7 activity assay in G361 cell lysates treated with varying doses of **43** for 24 h. The activities of caspases were measured using the fluorogenic substrate Ac-DEVD-AMC and normalized against an untreated control.

phosphorylation of known CDK substrates. When G361 cells were treated with **43** for 4 h, the abundance of the phospho-forms of Rb, protein phosphatase PP1alpha and nucleophosmin (NPM) decreased (Fig. 8c).

2.7. Induction of apoptosis

Besides measuring antiproliferative activity of compounds **43** we also evaluated in a detail the ability of **43** to induce apoptosis in G361 cells by imunoblotting and caspase activity assay. As shown in Fig. 9A, compound **43** influenced mitochondrial pathway of apoptosis in treated cells as documented by a decrease of pro-survival protein Mcl-1 and an increase of proapoptotic proteins Bax, Bak and Bid. Dose-dependent response has clearly correlated with observations of i) cellular level of zymogenes of effector caspases 3 and 7, ii) their active fragments and iii) cleavage of substrate, PARP (poly-ADP ribose polymerase). In addition, the activation of caspases was confirmed by an enzyme activity assay using fluorescently labeled substrates of caspases 3 and 7 (Fig. 9B).

3. Conclusion

In summary, thanks to a convergent synthesis pattern, 24 pyrrolo[2,3-*b*]pyridine based derivatives (**21**–**44**) were synthesized in 5–10 steps, with moderate to very good yields. The key step [3 + 2] cycloaddition reaction allowed us to enlarge our library of triheterocycles by giving us the opportunity to make 1,4- and 1,5-disubstituted triazoles. All the compounds were evaluated for *in vitro* inhibitory activity against CDK2/cyclin E and antiproliferative activity on cancer cell lines. Interestingly, some of them showed a single digit micro-molar inhibitory activity towards CDK2/cyclin E. From known CKIs from the literature, a 3D-QSAR CoMFA model was built and validated with good statistical results. This model gave us a correct prediction of the biological activity of our potent compounds towards CDK2/cyclin E and the contour map obtained will be of great use for improving our CKIs through a pharmacomodulation process.

Among the most potent compounds, the derivative **43**, containing a 1,5-disubstituted triazole, was found to be a pan-specific inhibitor of CDKs. The binding mode of **43** in CDK2 cavity have been described by molecular docking study and revealed donor-acceptor pattern of interaction of 7-azaindole ring with the main chain of Glu81 and Leu83. Cellular inhibition of CDK2 was confirmed by the monitoring of changes in the phosphorylation of known CDK substrates, Rb, PP1alpha and NPM.

Antiproliferative activity of **43** was studied in detail on G361 and MCF-7 cell lines and revealed a decrease of DNA replication and proliferation and a cell accumulation in G1 and G2/M phases in treated cells as it was previously described for numerous other pan-selective CDK inhibitors. In parallel, compound **43** showed to induce apoptosis in treated cells as it was documented by flow cytometry (subG1 population), imunoblot analysis of cleaved PARP and caspase activity assay.

4. Experimental section

4.1. Material and methods

All commercial materials were used without further purification. For anhydrous and inert reactions, the glassware was dried in an oven and several vacuum–nitrogen cycles were performed beforehand. The thin layer chromatography (TLC) studies were performed using commercial pre-coated aluminium sheets silica gel (60 Å, F_{254}) marketed by Merk. The purifications by chromatography on silica gel columns were carried out on an ISCO purification unit, Combi Flash RF 75 PSI, with Redisep flash silica gel columns (60 Å, 230–400 mesh, grade 9385). Purities of compounds were assessed by inspection of their proton and carbon nuclear magnetic resonance spectroscopy (^{1}H and ^{13}C NMR) spectra and high resolution mass spectrometry (HRMS) specta. NMR spectra were measured on a Brücker Ultrashield 300 spectrometer, 300 MHz (^{1}H) and 75 MHz (^{13}C) in deuterated chloroform ($CDCl_3$) or dimethylsulfoxide (DMSO-d_6). The notations used are: δ: chemical shift (ppm), s: singlet; d: doublet; dd: doublet of doublet; t: triplet; m:

multiplet; br: broad signal; *J*: coupling constant (Hz). The HRMS was performed by the mass spectrometry service on a Q-Exactive spectrometer from Thermo Scientific using the electrospray ionisation (ESI) technique. From known CKIs from the literature, a 3D-QSAR CoMFA model was built and validated with good statistical results. This model gave us a correct prediction of the biological activity of our potent compounds towards CDK2/cyclin E and the contour map obtained will be of great use for improving our CKIs through a pharmacomodulation process.

4.2. Synthesis of compounds 2–20

4.2.1. 3-Iodo-1H-pyrrolo[2,3-b]pyridine (**2**)

1*H*-Pyrrolo[2,3-*b*]pyridine 1 (1.00 g, 8.47 mmol) was dissolved in ethanol (40 mL) then iodine (3.23 g, 12.71 mmol), potassium iodide (2.11 g, 12.71 mmol) and a sodium hydroxide solution (12.71 mL, 12.71 mmol, 1 M) were added. The mixture was stirred overnight at room temperature. The reaction mixture was diluted with water and extracted with ethyl acetate (3 times). The organic layers were gathered, washed with a thiosulfate solution (w/w 5%) (twice) and a saturated sodium chloride solution, dried over magnesium sulfate, filtered and concentrated to give an orange solid. The crude product was recrystallised in methanol and water to give 2.00 g of the pure expected product as an orange solid in 97% yield. ^{1}H NMR (300 MHz, DMSO-d_6) δ (ppm): 12.11 (br, 1H), 8.26 (dd, J = 1.5, 4.8 Hz, 1H), 7.72 (d, J = 2.7 Hz, 1H), 7.69 (dd, J = 1.5, 7.8 Hz, 1H), 7.16 (dd, J = 4.8, 7.8 Hz, 1H). ^{13}C NMR (75 MHz, DMSO-d_6) δ (ppm): 148.5, 144.2, 130.9, 128.5, 122.4, 116.9, 54.8.

4.2.2. 3-((trimethylsilyl)ethynyl)-1H-pyrrolo[2,3-b]pyridine (**3a**)

General procedure for the Sonogashira cross-coupling reaction. Compound **2** (1.5 g, 6.15 mmol), copper iodide (118 mg, 0.62 mmol), bis(triphenylphosphine)palladium(II) dichloride (217 mg, 0.31 mmol), triethylamine (1.28 mL, 9.23 mmol), ethynyl(trimethyl) silane (1.30 mL, 9.23 mmol) and THF (35 mL) were introduced in an oven dried round bottom flask under inert atmosphere. The mixture was stirred at room temperature for 20 h. The reaction mixture was diluted with EtOAc and filtered on Dicalite. The filtrate was washed with water and a saturated solution of sodium chloride, dried over magnesium sulfate, filtered and concentrated. The crude product was purified by chromatography on silica gel column, cyclohexane/EtOAc 7:3, to give 1.099 g of the clean expected product as a beige solid in 84% yield. ^{1}H NMR (300 MHz, DMSO-d_6) δ (ppm): 12.12 (br, 1H), 8.30 (dd, J = 1.5, 4.7 Hz, 1H), 7.93 (dd, J = 1.5, 7.8 Hz, 1H), 7.88 (d, J = 2.7 Hz, 1H), 7.18 (dd, J = 4.7, 7.8 Hz, 1H), 0.24 (s, 9H). ^{13}C NMR (75 MHz, DMSO-d_6) δ (ppm): 148.0, 144.4, 131.4, 127.6, 120.8, 117.0, 99.6, 95.5, 95.4, 0.7 (3C).

4.2.3. 3-Ethynyl-1H-pyrrolo[2,3-b]pyridine (**4a**)

Compound **3a** (181 mg, 0.85 mmol) was dissolved in anhydrous THF, TBAF in solution in THF (1.7 mL, 1.70 mmol, 1 M) was added and the mixture was stirred at room temperature for 2 h. The reaction mixture was diluted with EtOAc, washed with water and a saturated sodium chloride solution, dried over magnesium sulfate, filtered and concentrated under reduced pressure to give 125 mg of the expected product as a pale brown solid in quantitative yield. ^{1}H NMR (300 MHz, DMSO-d_6) δ (ppm): 12.08 (br, 1H), 8.29 (dd, J = 1.5, 4.9 Hz, 1H), 7.96 (dd, J = 1.5, 7.8 Hz, 1H), 7.86 (br s, 1H), 7.17 (dd, J = 4.9, 7.8 Hz, 1H), 4.12 (s, 1H). ^{13}C NMR (75 MHz, DMSO-d_6) δ (ppm): 148.0, 144.3, 131.3, 127.6, 120.8, 117.0, 94.8, 82.0, 77.8.

4.2.4. 1-(Phenylsulfonyl)-1H-pyrrolo[2,3-b]pyridine (**5**)

In a heat dried and nitrogen purged round bottom flask, 1*H*-pyrrolo[2,3-*b*]pyridine **1** (1.01 g, 8.58 mmol), tetrabutylammonium bromide (81 mg, 0.25 mmol), finely grounded sodium hydroxide (1.02 g, 25.41 mmol) and CH_2Cl_2 (20 mL) were mixed, stirred and cooled down to 0 °C in an ice bath, then benzene sulfonylchloride (1.35 mL, 10.59 mmol) was added slowly. The mixture was left to warm up to room temperature and stirred at this temperature for 1 h. The reaction was hydrolysed with water (20 mL) and extracted by CH_2Cl_2 (twice). The organic layer was washed with a saturated sodium chloride solution, dried over magnesium sulfate and concentrated under reduced pressure to give 2.38 g of a beige solid. The crude product was purified by chromatography on silica gel column, cyclohexane/EtOAc 7:3, to give 2.17 g of the pure expected product as a white solid in 99% yield. ^{1}H NMR (300 MHz, $CDCl_3$) δ (ppm): 8.45 (dd, J = 1.5, 4.8 Hz, 1H), 8.20 (d, J = 7.5 Hz, 2H), 7.86 (dd, J = 1.5, 7.8 Hz, 1H), 7.73 (d, J = 4.0 Hz, 1H), 7.57 (dd, J = 7.4 Hz, 1H), 7.52–7.47 (m, 2H), 7.19 (dd, J = 4.8, 7.8 Hz, 1H), 6.61 (d, J = 4.0 Hz, 1H). ^{13}C NMR (75 MHz, $CDCl_3$) δ (ppm): 144.7 (2C), 138.3, 134.1, 129.9, 129.1 (2C), 128.0 (2C), 126.5, 123.0, 119.0, 105.5.

4.2.5. 2-Iodo-1-(phenylsulfonyl)-1H-pyrrolo[2,3-b]pyridine (**6**)

In a heat dried and nitrogen purged tricol round bottom flask, **5** (1.00 g, 3.88 mmol) was dissolved in THF (40 mL). The solution was cooled down to −60 °C and LDA (2.33 mL, 4.66 mmol, 2 M in THF) was added. The mixture was left to stir at −60 °C for 15 min. Diiodine (1.97 g, 7.76 mmol) in solution in THF (10 mL) was added slowly. The mixture was left to warm up to room temperature overnight and the reaction was quenched with water (25 mL). The mixture was diluted with EtOAc, washed with a thiosulfate solution (w/w 5%), water and a saturated sodium chloride solution, dried over magnesium sulfate, filtered and concentrated under reduced pressure to give 1.8 g of a brown solid. The crude product, a mixture of **6** and a diiodinated derivative **6′**, was purified by flash chromatography on silica gel column, cyclohexane/EtOAc 85:15, to give 750 mg of the clean expected product **6** as a pale yellow solid in 50% yield, **6′** described below and a mixed fraction, both not quantified. ^{1}H NMR (300 MHz, $CDCl_3$) δ (ppm): 8.55 (dd, J = 1.5, 4.8 Hz, 1H), 8.22 (d, J = 7.2 Hz, 2H), 7.79 (dd, J = 1.6, 7.8 Hz, 1H), 7.58 (dd, J = 7.3 Hz, 1H), 7.52–7.43 (m, 2H), 7.20 (dd, J = 4.8, 7.8 Hz, 1H), 6.83 (s, 1H). ^{13}C NMR (75 MHz, $CDCl_3$) δ (ppm): 149.7, 144.8, 138.8, 134.3, 129.2 (2C), 128.3 (2C), 127.9, 124.0, 120.4, 119.5, 76.4.

4.2.6. 2-Iodo-1-((2-iodophenyl)sulfonyl)-1H-pyrrolo[2,3-b] pyridine (**6′**)

^{1}H NMR (300 MHz, $CDCl_3$) δ (ppm): 8.55 (dd, J = 1.6, 8.0 Hz, 1H), 8.07 (dd, J = 1.6, 4.8 Hz, 1H), 7.93 (dd, J = 1.2, 7.8 Hz, 1H), 7.74 (dd, J = 1.6, 7.8 Hz, 1H), 7.58 (ddd, J = 1.2, 7.4, 8.0 Hz, 1H), 7.22 (ddd, J = 1.6, 7.8, 7.8 Hz, 1H), 7.08 (dd, J = 4.8, 7.8 Hz, 1H), 7.05 (s, 1H). ^{13}C NMR (75 MHz, $CDCl_3$) δ (ppm): 153.7, 149.3, 144.2, 142.6, 141.9, 134.6, 134.2, 128.1, 127.8, 123.5, 119.5, 119.3, 92.1.

4.2.7. 2-Iodo-1H-pyrrolo[2,3-b]pyridine (**7**)

In a heat dried and nitrogen purged round bottom flask, **5** (509 mg, 1.97 mmol) was dissolved in THF (20 mL). The solution was cooled down to −60 °C and LDA (1.97 mL, 3.95 mmol, 2 M in THF) was added. The mixture was left to stir at −60 °C for 15 min the diiodine (752 mg, 2.96 mmol) in solution in THF (10 mL) was added. The mixture was left to warm up to room temperature overnight and the reaction was quenched with water (5 mL). The mixture was diluted with EtOAc, washed with a thiosulfate solution (w/w, 5%), water and a saturated sodium chloride solution, dried over magnesium sulfate, filtered and concentrated under reduced pressure. The crude product was purified by flash chromatography on silica gel column, cyclohexane/EtOAc 85:15. A mixture of **6** and **6′** was obtained. This mixture was solubilised in dioxane (10 mL) and sodium *tert*-butoxide (380 mg, 3.95 mmol) was added. The mixture was left under stirring and reflux for 2 h. After being cooled down to room temperature, the reaction was quenched with water

(20 mL) and extracted with EtOAc. The organic layer was washed with a saturated sodium chloride solution, dried over magnesium sulfate, filtered and concentrated under reduced pressure to give 418 mg of the expected product as a pale orange solid in 87% yield. ^{1}H NMR (300 MHz, DMSO-d_6) δ (ppm): 12.19 (br, 1H), 8.28 (dd, J = 1.6, 4.7 Hz, 1H), 7.95 (dd, J = 1.5, 7.9 Hz, 1H), 7.09 (dd, J = 4.7, 7.9 Hz, 1H), 6.77 (sd, J = 1.6 Hz, 1H). ^{13}C NMR (75 MHz, DMSO-d_6) δ (ppm): 155.7, 147.7, 131.7, 126.9, 121.1, 114.8, 85.9.

4.2.8. 1-(Phenylsulfonyl)-2-((trimethylsilyl)ethynyl)-1H-pyrrolo[2,3-b]pyridine (**3b**)

Compound **3b** was synthesized following the general procedure for the Sonogashira coupling reaction from **6**. The crude product was purified by chromatography on silica gel column, cyclohexane/EtOAc 8:2, to give 285 mg of the expected product as a yellow oil (purity 70%), 46% calculated yield. ^{1}H NMR (300 MHz, $CDCl_3$) δ (ppm): 8.53 (dd, J = 1.5, 4.7 Hz, 1H), 8.21 (d, J = 7.3 Hz, 2H), 7.79 (dd, J = 1.5, 7.9 Hz, 1H), 7.58 (dd, J = 7.3 Hz, 1H), 7.53–7.43 (m, 2H), 7.20 (dd, J = 4.8, 7.9 Hz, 1H), 6.83 (s, 1H), 0.35 (s, 9H). ^{13}C NMR (75 MHz, DMSO-d_6) δ (ppm): 148.3, 146.4, 139.3, 134.1, 129.4, 129.1 (2C), 128.0 (2C), 121.4, 121.3, 119.7, 114.2, 105.0, 94.6, −0.25 (3C).

4.2.9. 2-((Trimethylsilyl)ethynyl)-1H-pyrrolo[2,3-b]pyridine (**3c**)

The derivative **3c** was synthesized following the general procedure for the Sonogashira coupling reaction from **7**. The crude product was purified by chromatography on silica gel column, cyclohexane/EtOAc 98:2, to give 381 mg of the clean expected product as an orange solid in 86% yield. ^{1}H NMR (300 MHz, DMSO-d_6) δ (ppm): 12.14 (brs, 1H), 8.27 (dd, J = 1.5, 4.7 Hz, 1H), 7.93 (ddd, J = 0.6, 1.5, 7.9 Hz, 1H), 7.09 (dd, J = 4.7, 7.9 Hz, 1H), 6.77 (sd, J = 2.0 Hz, 1H), 0.27 (s, 9H). ^{13}C NMR (75 MHz, DMSO-d_6) δ (ppm): 148.5, 145.2, 129.1, 119.6, 119.2, 116.9, 107.4, 99.2, 98.0, 0.2 (3C).

4.2.10. 2-Ethynyl-1H-pyrrolo[2,3-b]pyridine (**4b**)

Compound **3c** (331 mg, 1.55 mmol) was dissolved in THF (5 mL) and tetrabutylammonium fluoride (3.1 mL, 3.10 mmol, 1 M) was added. The mixture was stirred at room temperature for 2 h. The reaction mixture was diluted with EtOAc, washed with water and a saturated sodium chloride solution, dried over magnesium sulfate, filtered and concentrated. The crude product was purified by chromatography on silica gel column, cyclohexane/EtOAc 98:2–7:3, to give 149 mg of the clean expected product as a beige solid in 68% yield. ^{1}H NMR (300 MHz, DMSO-d_6) δ (ppm): 12.20 (br, 1H), 8.28 (dd, J = 1.6, 4.7 Hz, 1H), 7.95 (dd, J = 1.6, 7.9 Hz, 1H), 7.09 (dd, J = 4.7, 7.9 Hz, 1H), 6.77 (s, 1H), 4.58 (s, 1H). ^{13}C NMR (75 MHz, DMSO-d_6) δ (ppm): 148.5, 145.0, 129.0, 119.6, 118.8, 116.8, 107.0, 85.4, 76.9.

4.2.11. 2-Chloro-1-(1H-pyrrolo[2,3-b]pyridin-3-yl)ethanone (**9a**)

In a heat dried and nitrogen purged round bottom flask, aluminium chloride (3.99 g, 30.0 mmol) and CH_2Cl_2 (300 mL) were mixed and stirred at room temperature for 5 min then **1** (714 mg, 6.05 mmol) was added. The mixture was stirred for 1.5 h then cooled in an ice bath and chloroacetyl chloride (2.39 mL, 30.0 mmol) was added slowly. The reaction mixture was left to warm up to room temperature and left to stir overnight (16 h) at room temperature under nitrogen atmosphere. The mixture was cooled in an ice bath and quenched by MeOH (60 mL). The solvents were removed under reduced pressure and a saturated sodium bicarbonate solution (120 mL) was added to the resulting mixture which was then extracted three times by EtOAc. The gathered organic layers were washed with a saturated sodium chloride solution, dried over magnesium sulfate, filtered and concentrated under reduced pressure to give 1.01 g of a beige solid. The solid was triturated in CH_2Cl_2 and filtered to give 648 mg of the pure expected product as a pale beige solid in 55% yield. ^{1}H NMR (300 MHz, DMSO-d_6) δ (ppm): 12.68 (br, 1H), 8.60 (s, 1H), 8.46 (dd, J = 1.8, 7.8 Hz, 1H), 8.36 (dd, J = 1.8, 4.8 Hz, 1H), 7.29 (dd, J = 4.8, 7.8 Hz, 1H), 4.94 (s, 2H). ^{13}C NMR (75 MHz, DMSO-d_6) δ (ppm): 186.9, 149.4, 145.1, 135.6, 130.0, 118.9, 118.2, 112.8, 46.7.

4.2.12. 3-Chloro-1-(1H-pyrrolo[2,3-b]pyridin-3-yl)propan-1-one (**9b**)

In a heat dried and nitrogen purged round bottom flask, aluminium chloride (3.225 g, 25.40 mmol) and CH_2Cl_2 (100 mL) were mixed and stirred at room temperature for 5 min then **1** (600 mg, 5.08 mmol) was added. The mixture was stirred for 1.5 h then cooled in an ice bath and 3-chloropropionyl chloride (2.42 mL, 25.40 mmol) was added slowly. The reaction mixture was left to warm up to room temperature and left to stir overnight (16 h) at rt under nitrogen atmosphere. The mixture was cooled in an ice bath and quenched by MeOH (15 mL). The solvents were removed under reduced pressure and a saturated sodium bicarbonate solution (120 mL) was added to the resulting mixture which was then extracted three times by EtOAc. The gathered organic layers were washed with a saturated sodium chloride solution, dried over magnesium sulfate, filtered and concentrated under reduced pressure to give 1.01 g of the expected product as a beige solid 95% yield. ^{1}H NMR (300 MHz, DMSO-d_6) δ (ppm): 12.57 (br, 1H), 8.58 (br s, 1H), 8.49 (dd, J = 1.8, 7.8 Hz, 1H), 8.34 (dd, J = 1.8, 4.8 Hz, 1H), 7.26 (dd, J = 4.8, 7.8 Hz, 1H), 3.96 (t, J = 6.3 Hz, 2H), 3.40 (t, J = 6.3 Hz, 2H). ^{13}C NMR (75 MHz, DMSO-d_6) δ (ppm): 192.2, 149.5, 144.8, 135.4, 130.0, 118.7, 118.1, 115.5, 41.3, 40.6.

4.2.13. 3-(2-Chloroethyl)-1H-pyrrolo[2,3-b]pyridine (**10a**)

DME (10 mL) was put in a heat dried and nitrogen purged round bottom flask and cooled in a ice bath to 0 °C, then aluminium chloride (685 mg, 5.15 mmol) and lithium aluminium hydride (1.08 mL, 2.58 mmol, 2.4 mol L^{-1}) are added slowly. **9a** (200 mg, 1.03 mmol) in solution in DME (10 mL) was added and the mixture was stirred and left to warm up to room temperature then stirred at room temperature for 18 h. The reaction is quenched with MeOH (10 mL), concentrated under reduced pressure, mixed with a saturated sodium hydrogenocarbonate solution and extracted with EtOAc. The organic layer was washed with a saturated sodium chloride solution, dried over magnesium sulfate and concentrated under reduced pressure to give 182 mg of the expected product as an orange solid in 98% yield. ^{1}H NMR (300 MHz, DMSO-d_6) δ (ppm): 11.47 (br, 1H), 8.19 (dd, J = 1.5, 4.8 Hz, 1H), 8.01 (dd, J = 1.5, 7.8 Hz, 1H), 7.37 (d, J = 2.4 Hz, 1H), 7.04 (dd, J = 4.8, 7.8 Hz, 1H), 3.86 (t, J = 7.4 Hz, 2H), 3.15 (t, J = 7.4 Hz, 2H). ^{13}C NMR (75 MHz, DMSO-d_6) δ (ppm): 148.9, 143.0, 127.1, 124.6, 119.6, 115.4, 110.2, 45.5, 28.9.

4.2.14. 3-(3-Chloropropyl)-1H-pyrrolo[2,3-b]pyridine (**10b**)

DME (20 mL) was put in a heat dried and nitrogen purged round bottom flask and cooled in a ice bath to 0 °C, then aluminium chloride (798 mg, 6.00 mmol) and lithium aluminium hydride (1.25 mL, 3.00 mmol, 2.4 mol L^{-1}) are added slowly. **9b** (250 mg, 1.20 mmol) in solution in DME (20 mL) was added and the mixture was stirred and left to warm up to room temperature then stirred at room temperature for 20 h. The reaction is quenched with MeOH (30 mL), concentrated under reduced pressure, mixed with a saturated sodium hydrogenocarbonate solution and extracted with EtOAc. The organic layer was washed with a saturated sodium chloride solution, dried over magnesium sulfate and concentrated under reduced pressure to give 237 mg of an orange oil. The crude product was purified by chromatography on silica gel column, cyclohexane/EtOAc 6:4, to give 218 mg of the expected product as a pale yellow solid in 94% yield. ^{1}H NMR (300 MHz, DMSO-d_6) δ (ppm): 11.38 (br, 1H), 8.19 (dd, J = 1.5, 4.5 Hz, 1H), 7.95 (dd, J = 1.5, 7.8 Hz, 1H), 7.27 (br s, 1H), 7.03 (dd, J = 4.5, 7.8 Hz, 1H), 3.66 (t,

J = 6.5 Hz, 2H), 2.82 (dd, J = 6.9, 7.5 Hz, 2H), 2.03–2.12 (m, 2H). ^{13}C NMR (75 MHz, DMSO-d_6) δ (ppm): 149.1, 142.9, 126.9, 123.5, 119.7, 115.3, 112.4, 45.5, 33.1, 22.3.

4.2.15. 3-(2-Azidoethyl)-1H-pyrrolo[2,3-b]pyridine (**11a**)

Compound **10a** (178 mg, 0.99 mmol), sodium azide (322 mg, 4.95 mmol), DMF (5 mL) and water (2.5 mL) were mixed and stirred at 60 °C for 16 h. The mixture was cooled to room temperature, diluted with water and extracted three times with EtOAc. The organic layer was washed three times with a saturated sodium chloride solution, dried over magnesium sulfate, filtered and concentrated to give 190 mg of a brown oil. The crude product was purified by chromatography on silica gel column, cyclohexane/EtOAc 1:1, to give 141 mg of the expected product as a beige solid in 71% yield. ^{1}H NMR (300 MHz, DMSO) δ (ppm): 11.46 (br, 1H), 8.20 (dd, J = 1.8, 4.5 Hz, 1H), 8.01 (dd, J = 1.8, 7.8 Hz, 1H), 7.35 (d, J = 2.4 Hz, 1H), 7.04 (dd, J = 4.5, 7.8 Hz, 1H), 3.60 (t, J = 7.0 Hz, 2H), 2.97 (t, J = 7.0 Hz, 2H). ^{13}C NMR (75 MHz, DMSO) δ (ppm): 149.2, 143.0, 127.1, 124.3, 119.7, 115.4, 110.2, 51.4, 25.0.

4.2.16. 3-(3-Azidopropyl)-1H-pyrrolo[2,3-b]pyridine (**11b**)

Compound **10b** (195 mg, 1.00 mmol), sodium azide (325 mg, 5.00 mmol), DMF (5 mL) and water (2.5 mL) were mixed and stirred at 60 °C for 16 h. The mixture was cooled to room temperature, diluted with water and extracted three times with EtOAc. The organic layer was washed three times with a saturated sodium chloride solution, dried over magnesium sulfate, filtered and concentrated to give 198 mg of the expected product as a yellow oil 99% yield. ^{1}H NMR (300 MHz, DMSO-d_6) δ (ppm): 11.37 (br, 1H), 8.18 (dd, J = 1.5, 4.7 Hz, 1H), 7.94 (dd, J = 1.5, 7.8 Hz, 1H), 7.27 (br s, 1H), 7.03 (dd, J = 4.7, 7.8 Hz, 1H), 3.37 (t, J = 6.9 Hz, 2H), 2.75 (dd, J = 7.2, 7.8 Hz, 2H), 1.85–1.95 (ddd, J = 6.6, 6.9, 7.2, 7.8 Hz, 2H). ^{13}C NMR (75 MHz DMSO-d_6) δ (ppm): 149.1, 142.9, 126.9, 123.4, 119.7, 115.3, 112.7, 50.8, 29.4, 22.3.

4.2.17. 2-Azido-1-(1H-pyrrolo[2,3-b]pyridin-3-yl)ethanone (**12a**)

9a (50 mg, 0.26 mmol), sodium azide (85 mg, 1.30 mmol), DMF (2 mL) and water (1 mL) were mixed and stirred at room temperature for 36 h. The mixture was diluted with water (20 mL) and extracted three times by EtOAc. The gathered organic layers were washed twice with a saturated sodium chloride solution, dried over magnesium sulfate, filtered and concentrated under reduced pressure to give 51 mg of the pure expected product as a white solid in 98% yield. ^{1}H NMR (300 MHz, DMSO-d_6) δ (ppm): 12.66 (br, 1H), 8.53 (s, 1H), 8.47 (dd, J = 1.8, 7.8 Hz, 1H), 8.36 (dd, J = 1.8, 4.8 Hz, 1H), 7.29 (dd, J = 4.8, 7.8 Hz, 1H), 4.66 (s, 2H). ^{13}C NMR (75 MHz, DMSO-d_6) δ (ppm): 189. 8, 149.4, 145.0, 135.2, 129.9, 118.9, 118.0, 112.7, 54.2.

4.2.18. 3-Azido-1-(1H-pyrrolo[2,3-b]pyridin-3-yl)propan-1-one (**12b**)

Compound **9b** (238 mg, 1.14 mmol) was dissolved in DMF (5 mL) then sodium azide (371 mg, 5.70 mmol) in solution in water (2.5 mL) was added. The mixture was stirred at 60 °C overnight (16 h) then poured onto ice and extracted three times with EtOAc. The gathered organic layers were washed twice with a saturated sodium chloride solution, dried over magnesium sulfate, filtered and concentrated under reduced pressure to give 282 mg a yellow solid. The crude product was purified by chromatography on silica gel column, CH_2Cl_2/EtOAc 7:3, to give 146 mg of the expected product as a white solid in 60% yield. ^{1}H NMR (300 MHz, DMSO-d_6) δ (ppm): 12.56 (br, 1H), 8.57 (s, 1H), 8.48 (dd, J = 1.8, 7.8 Hz, 1H), 8.33 (dd, J = 1.8, 4.8 Hz, 1H), 7.26 (dd, J = 4.8, 7.8 Hz, 1H), 3.68 (t, J = 6.3 Hz, 2H), 3.22 (t, J = 6.3 Hz, 2H). ^{13}C NMR (75 MHz, DMSO-d_6) δ (ppm): 193.1, 149.4, 144.8, 135.2, 130.0, 118.6, 118.0, 115.3, 46.7, 37.9.

4.2.19. 3-Bromo-1H-pyrrolo[2,3-b]pyridine (**13**)

In a heat dried and nitrogen purged round bottom flask, **1** (1.00 g, 8.46 mmol) was dissolved in CH_2Cl_2 (20 mL) and cooled in an ice bath, then *N*-bromosuccinimide (1.66 g, 9.31 mmol) was added. The mixture was left to warm up to room temperature overnight under nitrogen atmosphere. The reaction mixture was diluted with CH_2Cl_2 and washed with a saturated sodium hydrogenocarbonate solution. The aqueous layer was extracted three times with EtOAc and the gathered organic layers were washed with a saturated sodium chloride solution, dried over magnesium sulfate, filtered and concentrated to give 1.79 g of a brown solid. The crude product was purified by chromatography on silica gel column, cyclohexane/EtOAc 1:1, to give 1.56 g of the expected product as a light brown solid in 93% yield. ^{1}H NMR (300 MHz, DMSO-d_6) δ (ppm): 11.45 (br, 1H), 8.38 (dd, J = 1.2, 5.1 Hz, 1H), 8.06 (dd, J = 1.2, 7.8 Hz, 1H), 7.48 (s, 1H), 7.28 (dd, J = 5.1, 7.8 Hz, 1H). ^{13}C NMR (75 MHz, DMSO-d_6) δ (ppm): 145.0, 140.9, 130.2, 125.6, 121.5, 116.3, 89.9.

4.2.20. 3-Bromo-1-(phenylsulfonyl)-1H-pyrrolo[2,3-b]pyridine (**14**)

In a heat dried and nitrogen purged round bottom flask, **13** (175 mg, 0.89 mmol), tetrabutylammonium bromide (10 mg, 0.03 mmol), finely grounded sodium hydroxide (107 mg, 2.67 mmol) and CH_2Cl_2 (5 mL) were mixed, stirred and cooled down to 0 °C in an ice bath, then benzene sulfonyl chloride (0.142 mL, 1.11 mmol) was added slowly. The mixture was left to warm up to room temperature and was stirred at this temperature for 1 h. The reaction was hydrolyzed with water (6 mL) and extracted by CH_2Cl_2 (twice). The organic layer was washed with water and a saturated sodium chloride solution, dried over magnesium sulfate and concentrated under reduced pressure to give an orange solid. The crude product was triturated in pentane, filtered, washed with pentane and dried to give 294 mg of the expected product as an orange solid in 98% yield. ^{1}H NMR (300 MHz, $CDCl_3$) δ (ppm): 8.48 (dd, J = 1.5, 4.8 Hz, 1H), 8.24–8.17 (m, 2H), 7.82 (dd, J = 1.5, 8.0 Hz, 1H), 7.79 (s, 1H), 7.60 (dd, J = 7.5 Hz, 1H), 7.54–7.46 (m, 2H), 7.27 (dd, J = 4.8, 8.0 Hz, 1H). ^{13}C NMR (75 MHz, $CDCl_3$) δ (ppm): 146.0 (2C), 138.0, 134.3, 129.2 (2C), 128.6, 128.1 (2C), 125.0, 122.5, 119.5, 95.6.

4.2.21. 3-Methyl-1-(phenylsulfonyl)-1H-pyrrolo[2,3-b]pyridine (**15**)

In a heat dried and nitrogen purged round bottom flask, **14** (1.064 g, 3.16 mmol) and tetrakis triphenylphosphine palladium (183 mg, 0.16 mmol) were dissolved in anhydrous THF (20 mL) then trimethylaluminium (3.17 mL, 6.32 mmol, 2.0 mol L^{-1}) was added slowly. The mixture was stirred at 60 °C for 16 h then cooled down to room temperature, diluted with a saturated sodium hydrogenocarbonate solution and extracted by EtOAc three times. The organic layers were gathered, washed with a saturated sodium chloride solution, dried over magnesium sulfate, filtered and concentrated to give 1.157 g of a red solid. The crude product was purified by chromatography on silica gel column, cyclohexane/EtOAc 8:2, to give 782 mg of the expected product as a yellow solid in 91% yield. ^{1}H NMR (300 MHz, $CDCl_3$) δ (ppm): 8.43 (dd, J = 1.5, 4.8 Hz, 1H), 8.20–8.12 (m, 2H), 7.78 (dd, J = 1.5, 7.8 Hz, 1H), 7.55 (dd, J = 7.1, 7.5 Hz, 1H), 7.50–7.42 (m, 4H), 7.18 (dd, J = 4.8, 7.8 Hz, 1H), 2.25 (sd, J = 1.3 Hz, 3H). ^{13}C NMR (75 MHz, $CDCl_3$) δ (ppm): 144.7 (2C), 138.6, 133.8, 129.0 (2C), 128.0, 127.8 (2C), 124.1, 123.2, 118.6, 115.1, 9.8.

4.2.22. 3-(Azidomethyl)-1-(phenylsulfonyl)-1H-pyrrolo[2,3-b] pyridine (**16**)

In a heat dried and nitrogen purged round bottom flask, **15**

(574 mg, 2.11 mmol), *N*-bromosuccinimide (413 mg, 2.32 mg), azobisisobutyronitrile (13 mg, 0.08 mmol) and carbon tetrachloride (10 mL) were mixed and stirred under reflux for 16 h. The reaction mixture was cooled to room temperature, and concentrated under reduced pressure. The crude product (brown oil), sodium azide (686 mg, 10.55 mmol), DMF (15 mL) and water (7.5 mL) were mixed and stirred at 60 °C for 16 h. The mixture was cooled to room temperature, diluted with water and extracted three times with EtOAc. The organic layer was washed three times with a saturated sodium chloride solution, dried over magnesium sulfate, filtered and concentrated to give a yellow oil. The crude product was purified by chromatography on silica gel column, cyclohexane/EtOAc 8:2 to give 377 mg of the expected product as a white solid in 57% yield. ^{1}H NMR (300 MHz, $CDCl_3$) δ (ppm): 8.48 (dd, J = 1.6, 4.8 Hz, 1H), 8.23–8.16 (m, 2H), 7.91 (dd, J = 1.6, 7.9 Hz, 1H), 7.76 (s, 1H), 7.59 (dd, J = 7.5 Hz, 1H), 7.54–7.45 (m, 2H), 7.23 (dd, J = 4.8, 7.9 Hz, 1H), 4.46 (s, 2H). ^{13}C NMR (75 MHz, $CDCl_3$) δ (ppm): 147.4, 145.7, 138.1, 134.2, 129.1 (2C), 128.3, 128.1 (2C), 124.9, 121.6, 119.4, 113.5, 46.2.

*4.2.23. 1-(Phenylsulfonyl)-1H-pyrrolo[2,3-b]pyridine-2-carboxylic acid (**17**)*

In a heat dried and nitrogen purged tricol round bottom flask, **5** (1.05 g, 4.07 mmol) was solubilized in dry THF (15 mL), cooled to −35 °C then lithium diisopropylamide (5.1 mL, 10.16 mmol, 2 M) was added slowly. The mixture was then cooled to −55 °C and dry ice was added slowly. The mixture was left to warm up to room temperature under stirring overnight. The reaction was quenched with water and extracted with EtOAC. The aqueous layer was acidified by the addition of a 6 N hydrochloric acid solution to pH = 1 and extracted with EtOAC. The latter organic layer was washed with a saturated sodium chloride solution, dried over magnesium sulfate, filtered and concentrated under reduced pressure to give 1.09 g of the expected product as a beige solid in 88% yield. ^{1}H NMR (300 MHz, DMSO-d_6) δ (ppm): 13.87 (br, 1H), 8.51 (dd, J = 1.6, 4.7 Hz, 1H), 8.26 (d, J = 7.0 Hz, 2H), 8.13 (dd, J = 1.6, 7.9 Hz, 1H), 7.77 (dd, J = 7.2 Hz, 1H), 7.72–7.65 (m, 2H), 7.39 (dd, J = 4.7, 7.9 Hz, 1H), 7.28 (s, 1H). ^{13}C NMR (75 MHz, DMSO-d_6) δ (ppm): 164.4, 149.5, 147.3, 138.5, 135.1, 133.3, 132.1, 129.8 (2C), 128.3 (2C), 121.1, 120.7, 112.5.

*4.2.24. Ethyl 1H-pyrrolo[2,3-b]pyridine-2-carboxylate (**18**)*

Compound **17** (302 mg, 1.00 mmol), EtOH (20 mL) and concentrated sulfuric acid (0.2 mL) were mixed in a round bottom flask and stirred under reflux for 20 h. The reaction mixture was cooled to room temperature and concentrated under reduced pressure. The residue was solubilized in EtOAc and washed three times with a saturated sodium hydrogenocarbonate solution, washed with water and a saturated sodium chloride solution, dried over magnesium sulfate, filtered and concentrated under reduced pressure. The crude product was purified by chromatography on silica gel column, CH_2Cl_2/EtOAc 8:2, to give 178 mg of the expected product as a white solid in 94% yield. ^{1}H NMR (300 MHz, DMSO-d_6) δ (ppm): 12.49 (br, 1H), 8.41 (dd, J = 1.7, 4.6 Hz, 1H), 8.11 (dd, J = 1.6, 8.0 Hz, 1H), 7.17 (s, 1H), 7.16 (dd, J = 4.6, 8.0 Hz, 1H), 3.34 (q, J = 7.1 Hz, 2H), 1.34 (t, J = 7.1 Hz, 3H). ^{13}C NMR (75 MHz, DMSO-d_6) δ (ppm): 161.5, 149.3, 147.2, 131.2, 128.3, 119.5, 117.3, 106.9, 61.1, 14.7.

*4.2.25. (1H-Pyrrolo[2,3-b]pyridin-2-yl)methanol (**19**)*

Dimethoxyethane (10 mL) was placed in a dry round bottom flask under nitrogen atmosphere and cooled to 0 °C. Lithium aluminium hydride (1.53 mL, 3.66 mmol, 2.4 M) then **18** (348 mg, 1.83 mmol) in solution in dimethoxyethane (10 mL) were added. The mixture was left to slowly warm up to room temperature under stirring overnight. The reaction was quenched with MeOH (15 mL) and the mixture was concentrated under reduced pressure. The residue was solubilized in EtOAc, washed with a saturated sodium hydrogenocarbonate solution, water and a saturated sodium chloride solution, dried over magnesium sulfate, filtered and concentrated under reduced pressure to give 113 mg of the expected product as a pale yellow solid in 94% yield. ^{1}H NMR (300 MHz, DMSO-d_6) δ (ppm): 11.51 (br, 1H), 8.13 (dd, J = 1.5, 4.7 Hz, 1H), 7.85 (dd, J = 1.5, 7.8 Hz, 1H), 7.00 (dd, J = 4.7, 7.8 Hz, 1H), 6.29 (s, 1H), 5.28 (t, J = 5.0 Hz, 1H), 4.60 (d, J = 5.0 Hz, 2H). ^{13}C NMR (75 MHz, DMSO-d_6) δ (ppm): 149.2, 142.3, 141.6, 127.9, 120.5, 115.8, 97.5, 57.4.

*4.2.26. 2-(Azidomethyl)-1H-pyrrolo[2,3-b]pyridine (**20**)*

In a heat dried and nitrogen purged round bottom flask, **19** (311 mg, 2.10 mmol) and CH_2Cl_2 (10 mL) were mixed then thionyl chloride (0.184 mL, 2.52 mmol) was added. The mixture was stirred at room temperature for 1 h then concentrated under reduced pressure. The crude product was mixed with sodium azide (683 mg, 10.50 mmol), DMF (10 mL) and water (5 mL). The mixture was stirred at 60 °C overnight. The reaction mixture was poured onto ice and extracted three times with EtOAc. The organic layers were gathered and washed three times with a saturated sodium chloride solution, dried over magnesium sulfate, filtered and concentrated. The crude product was purified by chromatography on silica gel column, cyclohexane/EtOAc 7:3, to give 252 mg of the expected product as an off white solid in 69%. ^{1}H NMR (300 MHz, DMSO-d_6) δ (ppm): 11.86 (br, 1H), 8.21 (dd, J = 1.6, 4.7 Hz, 1H), 7.94 (dd, J = 1.5, 7.8 Hz, 1H), 7.06 (dd, J = 4.7, 7.8 Hz, 1H), 6.49 (sd, J = 1.9 Hz, 1H), 4.58 (s, 2H). ^{13}C NMR (75 MHz, DMSO-d_6) δ (ppm): 149.3, 143.5, 134.2, 128.7, 120.2, 116.3, 100.6, 47.6.

4.3. Synthesis of compounds 21–33. General procedure for the copper-catalyzed [3 + 2] cycloaddition reaction

*4.3.1. 3-(2-(4-(1H-pyrrolo[2,3-b]pyridin-3-yl)-1H-1,2,3-triazol-1-yl)ethyl)-1H-pyrrolo[2,3-b]pyridine (**21**)*

In a heat dried and nitrogen purged round bottom flask, **3a** (58 mg, 0.27 mmol), **11a** (50 mg, 0.27 mmol), copper iodide (1.4 mg, 0.03 mmol) and THF (5 mL) were mixed and stirred then tetrabutylammonium fluoride (0.81 mL, 0.81 mmol, 1 M) and diisopropylethylamine (0.092 mL, 0.54 mmol) were added. The mixture was stirred at 40 °C for 16 h. The reaction mixture was cooled to room temperature, concentrated and purified by chromatography on silica gel column, CH_2Cl_2/MeOH 95:5, to give 125 mg of a brown oil which was triturated in MeOH/diethylether to give 61 mg of the expected product as a beige solid in 69% yield. ^{1}H NMR (300 MHz, DMSO-d_6) δ (ppm): 11.87 (br, 1H), 11.42 (br, 1H), 8.47 (s, 1H), 8.37 (dd, J = 1.2, 8.0 Hz, 1H), 8.28 (dd, J = 1.5, 4.7 Hz, 1H), 8.18 (dd, J = 1.5, 4.7 Hz, 1H), 7.99 (dd, J = 1.1, 7.9 Hz, 1H), 7.85 (sd, J = 2.6 Hz, 1H), 7.25 (d, J = 2.4 Hz, 1H), 7.16 (dd, J = 4.7, 8.0 Hz, 1H), 7.03 (dd, J = 4.7, 7.9 Hz, 1H), 4.70 (t, J = 7.3 Hz, 2H), 2.34–2.21 (m, 2H). ^{13}C NMR (75 MHz, DMSO-d_6) δ (ppm): 149.0, 148.9, 143.6, 143.0, 142.2, 128.7, 126.9, 124.2, 123.5, 120.2, 119.7, 117.5, 116.5, 115.5, 109.6, 105.7, 50.4, 26.4. HRMS-ESI (*m/z*): found 330.14636, calcd for $C_{18}H_{16}N_7$ $[M + H]^+$ 330.14617.

Compounds **22**–**36** were synthesized following the general procedure for the copper-catalysed cycloaddition reaction (with or without additives).

*4.3.2. 3-(2-(4-Phenyl-1H-1,2,3-triazol-1-yl)ethyl)-1H-pyrrolo[2,3-b]pyridine (**22**)*

Purification by chromatography on silica gel column, CH_2Cl_2/MeOH 98:2, to give 123 mg of the expected product as an off white solid in 80% yield. ^{1}H NMR (300 MHz, DMSO-d_6) δ (ppm): 11.42 (br, 1H), 8.57 (s, 1H), 8.20 (br, 1H), 7.97 (d, J = 7.2 Hz, 1H), 7.80 (d, J = 7.2 Hz, 2H), 7.44 (dd, J = 7.2 Hz, 1H), 7.32 (dd, J = 7.2 Hz, 1H), 7.24 (d, 1H, J = 2.1 Hz), 7.03 (dd, J = 4.8, 7.8 Hz, 1H), 4.69 (t, J = 7.2 Hz,

2H), 3.33 (t, J = 7.2 Hz, 2H). ^{13}C NMR (75 MHz, DMSO-d_6) δ (ppm): 148.9, 145.6, 143.0, 131.3, 129.4 (3C), 128.4, 126.9, 125.5 (2C), 124.3, 121.8, 109.5, 50.6, 26.3. HRMS-ESI (*m/z*): found 290.14018, calcd for $C_{17}H_{16}N_5$ $[M+H]^+$ 290.14002.

*4.3.3. 2-(4-(1H-Pyrrolo[2,3-b]pyridin-3-yl)-1H-1,2,3-triazol-1-yl)-1-(1H-pyrrolo[2,3-b]pyridin-3-yl)ethanone (**23**)*

Purification by chromatography on silica gel column, CH_2Cl_2/MeOH 9:1–8:2, to give 123 mg of the expected product as a brown solid not pure. The solid was tritutated in water, filtered, washed with diethyl ether and dried to give 44 mg of the expected product as a brown solid in 26% yield. ^{1}H NMR (300 MHz, DMSO-d_6) δ (ppm): 12.80 (br, 1H), 11.93 (br, 1H), 8.80 (d, J = 3.0 Hz, 1H), 8.50 (s, 1H), 8.59–8.42 (m, 2H), 8.42–8.20 (m, 2H), 7.97 (d, J = 2.1 Hz, 1H), 7.30 (dd, J = 4.8, 7.8 Hz, 1H), 7.19 (dd, J = 4.2, 7.8 Hz, 1H), 6.05 (s, 2H). ^{13}C NMR (75 MHz, DMSO-d_6) δ (ppm): 187.1, 149.4, 149.1, 145.2, 143.6, 142.5, 135.7, 134.5, 129.9, 128.8, 123.7, 122.1, 119.0, 118.1, 112.7, 105.7, 55.6. HRMS-ESI (*m/z*): found 344.12582, calcd for $C_{18}H_{14}N_7O$ $[M+H]^+$ 344.12543.

*4.3.4. 2-(4-Phenyl-1H-1,2,3-triazol-1-yl)-1-(1H-pyrrolo[2,3-b]pyridin-3-yl)ethanone (**24**)*

Purification by chromatography on silica gel column, CH_2Cl_2/MeOH 98:2, to give 52 mg of the expected product as a white solid in 68% yield. ^{1}H NMR (300 MHz, DMSO-d_6) δ (ppm): 12.80 (br, 1H), 8.79 (sd, J = 3.0 Hz, 1H), 8.61 (s, 1H), 8.43 (dd, J = 1.5, 7.8 Hz, 1H), 8.38 (dd, J = 1.5, 4.8 Hz, 1H), 7.89 (d, J = 7.6 Hz, 2H), 7.48 (dd, J = 7.3, 7.6 Hz, 2H), 7.35 (dd, J = 7.6 Hz, 1H), 7.30 (dd, J = 4.8, 7.8 Hz, 1H), 6.05 (s, 2H). ^{13}C NMR (75 MHz, DMSO-d_6) δ (ppm): 186.9, 149.4, 146.7, 145.2, 135.8, 131.3, 129.9, 129.4 (2C), 128.3, 125.6 (2C), 123.7, 119.0, 118.1, 112.6, 55.7. HRMS-ESI (*m/z*): found 304.11961, calcd for $C_{17}H_{14}N_5O$ $[M+H]^+$ 304.11929.

*4.3.5. 3-(3-(4-(1H-Pyrrolo[2,3-b]pyridin-3-yl)-1H-1,2,3-triazol-1-yl)propyl)-1H-pyrrolo[2,3-b]pyridine (**25**)*

Purification by chromatography on silica gel column, CH_2Cl_2/MeOH 9:1, to give 49 mg of the expected product as a beige solid not pure. The solid was triturated in THF, filtered, washed with THF and dried to give 30 mg of the expected product as a brown solid in 38% yield. ^{1}H NMR (300 MHz, DMSO-d_6) δ (ppm): 11.88 (br, 1H), 11.39 (br, 1H), 8.52 (s, 1H), 8.43 (dd, J = 1.2, 7.8 Hz, 1H), 8.28 (dd, J = 1.5, 4.8 Hz, 1H), 8.19 (dd, J = 1.5, 4.5 Hz, 1H), 7.95 (dd, J = 1.2, 7.8 Hz, 1H), 7.89 (d, J = 2.8 Hz, 1H), 7.32 (d, J = 2.1 Hz, 1H), 7.17 (dd, J = 4.8, 8.1 Hz, 1H), 7.03 (dd, J = 4.8, 7.8 Hz, 1H), 4.46 (t, J = 7.3 Hz, 2H), 2.74 (t, J = 7.3 Hz, 2H), 2.28 (td, J = 7.3 Hz, 2H). ^{13}C NMR (75 MHz, DMSO-d_6) δ (ppm): 149.2, 149.1, 143.6, 142.9, 142.4, 128.8, 127.0, 123.6 (2C), 120.2, 119.7, 117.5, 116.4, 115.3, 112.5, 105.7, 49.6, 30.7, 22.1. HRMS-ESI (*m/z*): found 344.16204, calcd for $C_{19}H_{18}N_7$ $[M+H]^+$ 344.16182.

*4.3.6. 3-(4-(1H-Pyrrolo[2,3-b]pyridin-3-yl)-1H-1,2,3-triazol-1-yl)-1-(1H-pyrrolo[2,3-b]pyridin-3-yl)propan-1-one (**26**)*

Purification by chromatography on silica gel column, CH_2Cl_2/MeOH 9:1–85:15, to give 93 mg of the expected product as an orange solid not pure. The solid was triturated in CH_2Cl_2, filtered, washed with diethyl ether and dried to give 77 mg of the expected product as a beige solid in 57% yield. ^{1}H NMR (300 MHz, DMSO-d_6) δ (ppm): 12.56 (br, 1H), 11.87 (br, 1H), 8.58 (s, 1H), 8.50 (s, 1H), 8.47 (dd, J = 1.5, 7.8 Hz, 1H), 8.39 (dd, J = 1.5, 7.8 Hz, 1H), 8.32 (dd, J = 1.5, 4.8 Hz, 1H), 8.27 (dd, J = 1.5, 4.8 Hz, 1H), 7.88 (sd, J = 2.8 Hz, 1H), 7.25 (dd, J = 4.8, 7.8 Hz, 1H), 7.16 (dd, J = 4.2, 7.8 Hz, 1H), 4.84–4.74 (m, 2H), 3.72–3.60 (m, 2H). ^{13}C NMR (75 MHz, DMSO-d_6) δ (ppm): 192.5, 149.4, 149.0, 144.8, 143.6, 142.3, 135.3, 130.0, 128.7, 123.6, 120.5, 118.7, 118.0, 117.5, 116.4, 115.2, 105.6, 45.5, (1C in the DMSO peak). HRMS-ESI (*m/z*): found 358.14171, calcd for $C_{19}H_{16}N_7O$ $[M+H]^+$ 358.14108.

*4.3.7. 3-((4-(1H-Pyrrolo[2,3-b]pyridin-3-yl)-1H-1,2,3-triazol-1-yl)methyl)-1-(phenylsulfonyl)-1H-pyrrolo[2,3-b]pyridine (**27**)*

Purification by chromatography on silica gel column, CH_2Cl_2/MeOH 98:2, to give 71 mg of the expected product as a white solid in 68% yield. ^{1}H NMR (300 MHz, DMSO-d_6) δ (ppm): 11.88 (br, 1H), 8.54 (s, 1H), 8.45–8.35 (m, 2H), 8.27 (dd, J = 1.6, 4.8 Hz, 1H), 8.19 (s, 1H), 8.15 (d, J = 7.2 Hz, 2H), 8.02 (dd, J = 1.6, 8.0 Hz, 1H), 7.88 (d, J = 2.6 Hz, 1H), 7.73 (dd, J = 7.5 Hz, 1H), 7.67–7.59 (m, 2H), 7.33 (dd, J = 4.8, 8.0, Hz, 1H), 7.16 (dd, J = 4.8, 7.9, Hz, 1H), 5.84 (s, 2H). ^{13}C NMR (75 MHz, DMSO-d_6) δ (ppm): 149.0, 147.1, 145.7, 143.7, 142.9, 137.8, 135.4, 130.1 (2C), 129.4, 128.8, 128.1 (2C), 126.5, 123.9, 121.7, 120.2, 120.0, 117.4, 116.5, 114.64, 105.4, 44.8. HRMS-ESI (*m/z*): found 456.12390, calcd for $C_{23}H_{18}N_7O_2S$ $[M+H]^+$ 456.12372.

*4.3.8. 3-(1-((1H-Pyrrolo[2,3-b]pyridin-2-yl)methyl)-1H-1,2,3-triazol-4-yl)-1H-pyrrolo [2,3-b]pyridine (**28**)*

Purification by chromatography on silica gel column, CH_2Cl_2/MeOH 95:5, to give 110 mg of the expected product as an orange solid not pure. The solid was triturated in water, filtered, washed with diethyl ether and dried to give 74 mg of the clean expected product as a brown solid in 59% yield. ^{1}H NMR (300 MHz, DMSO-d_6) δ (ppm): 11.96 (br, 1H), 11.89 (br, 1H), 8.52 (s, 1H), 8.44 (dd, J = 1.3, 7.9 Hz, 1H), 8.34–8.16 (m, 2H), 7.97–7.89 (m, 2H), 7.18 (dd, J = 4.7, 7.9 Hz, 1H), 7.06 (dd, J = 4.7, 7.8 Hz, 1H), 6.50 (sd, J = 1.7 Hz, 1H), 5.82 (s, 2H). ^{13}C NMR (75 MHz, DMSO-d_6) δ (ppm): 149.3, 149.1, 143.6, 143.5, 142.8, 134.3, 128.8, 123.8, 120.3, 117.5, 116.5, 116.4, 105.5, 100.6, 47.2. HRMS-ESI (*m/z*): found 316.13090, calcd for $C_{17}H_{14}N_7$ $[M+H]^+$ 316.13052.

*4.3.9. 2-(1-(2-(1H-Pyrrolo[2,3-b]pyridin-3-yl)ethyl)-1H-1,2,3-triazol-4-yl)-1-(phenylsulfonyl)-1H-pyrrolo[2,3-b]pyridine (**29**) and 3-(2-(4-(1H-pyrrolo[2,3-b]pyridin-2-yl)-1H-1,2,3-triazol-1-yl)ethyl)-1H-pyrrolo[2,3-b]pyridine (**30**)*

Purification by chromatography on silica gel column, CH_2Cl_2/MeOH 95:5, to give two fractions. Fraction 1: 87 mg of a brown solid not pure. The solid was triturated in diethyl ether, filtered, washed with diethyl ether and dried to give 80 mg of the expected product **29** as a brown solid in 43% yield. Fraction 2: 176 mg of a brown solid/oil not pure. The solid/oil was triturated in EtOAc/CH_2Cl_2/cyclohexanne, filtered, washed with CH_2Cl_2 and dried to give 51 mg of the product **30** as a pale pink solid in 39% yield.

*4.3.10. 2-(1-(2-(1H-Pyrrolo[2,3-b]pyridin-3-yl)ethyl)-1H-1,2,3-triazol-4-yl)-1-(phenylsulfonyl)-1H-pyrrolo[2,3-b]pyridine (**29**)*

^{1}H NMR (300 MHz, DMSO-d_6) δ (ppm): 12.19 (br, 1H), 8.45 (s, 1H), 8.34 (dd, J = 1.5, 4.8 Hz, 1H), 8.29–8.15 (br, 1H), 8.10 (dd, J = 1.5, 7.9 Hz, 1H), 7.99–7.89 (m, 3H), 7.72 (s, 1H), 7.60 (dd, J = 7.5 Hz, 1H), 7.47 (dd, J = 7.5, 8.0 Hz, 2H), 7.30 (dd, J = 4.8, 7.9 Hz, 1H), 7.08 (dd, J = 4.8, 7.9 Hz, 1H), 6.80 (s, 1H), 4.82 (t, J = 6.8 Hz, 2H), 3.40–3.30 (m, 2H). ^{13}C NMR (75 MHz, DMSO-d_6) δ (ppm): 149.9, 149.4, 147.1, 145.3, 143.3, 140.5, 137.8, 135.0, 130.4, 129.9 (2C), 129.2, 128.4, 128.3, 127.6 (2C), 124.8, 122.8, 122.3, 119.7, 116.0, 97.3, 49.4, 25.7. HRMS-ESI (*m/z*): found 470.13994, calcd for $C_{24}H_{20}N_7O_2S$ $[M+H]^+$ 470.13937.

*4.3.11. 3-(2-(4-(1H-Pyrrolo[2,3-b]pyridin-2-yl)-1H-1,2,3-triazol-1-yl)ethyl)-1H-pyrrolo[2,3-b]pyridine (**30**)*

^{1}H NMR (300 MHz, DMSO-d_6) δ (ppm): 12.13 (br, 1H), 11.43 (br, 1H), 8.41 (s, 1H), 8.19 (dd, J = 1.5, 4.8 Hz, 2H), 7.97 (dd, J = 1.5, 7.9 Hz, 1H), 7.93 (dd, J = 1.5, 7.9 Hz, 1H), 7.24 (sd, J = 2.4 Hz, 1H), 7.09–7.00 (m, 2H), 6.78 (sd, J = 2.0 Hz, 1H), 4.75 (t, J = 7.0 Hz, 2H), 3.39–3.29 (m, 2H). ^{13}C NMR (75 MHz, DMSO-d_6) δ (ppm): 149.5, 149.0, 143.2, 143.0, 140.4, 130.6, 128.3, 126.9, 124.4, 122.2, 120.9, 119.6, 116.4, 115.5, 109.4, 97.2, 50.6, 26.4. HRMS-ESI (*m/z*): found 330.14637,

calcd for $C_{18}H_{16}N_7$ $[M+H]^+$ 330.14617.

4.3.12. 2-(4-(1H-Pyrrolo[2,3-b]pyridin-2-yl)-1H-1,2,3-triazol-1-yl)-1-(1H-pyrrolo [2,3-b]pyridin-3-yl)ethanone (**31**)

The reaction mixture was cooled to room temperature and filtered. The solid was washed with THF and dried under reduced pressure to give 115 mg of the expected product as an off white solid in 84% yield. ^{1}H NMR (300 MHz, DMSO-d_6) δ (ppm): 12.81 (br, 1H), 12.26 (br, 1H), 8.80 (sd, J = 3.1 Hz, 1H), 8.55 (s, 1H), 8.44 (dd, J = 1.2, 7.9 Hz, 1H), 8.39 (d, J = 3.9 Hz, 1H), 8.32–8.15 (br, 1H), 7.97 (d, J = 7.9 Hz, 1H), 7.31 (dd, J = 4.8, 7.9 Hz, 1H), 7.15–7.02 (m, 1H), 6.89 (s, 1H), 6.13 (s, 2H). ^{13}C NMR (75 MHz, DMSO-d_6) δ (ppm): 186.9, 149.4 (2C), 145.2 (2C), 140.5, 135.8 (2C), 130.6, 129.9, 128.3, 124.0 (2C), 119.0, 118.1, 112.6, 97.4, 55.7. HRMS-ESI (*m/z*): found 344.12578, calcd for $C_{18}H_{14}N_7O$ $[M+H]^+$ 344.12543.

4.3.13. 2-(1-(3-(1H-Pyrrolo[2,3-b]pyridin-3-yl)propyl)-1H-1,2,3-triazol-4-yl)-1-(phenylsulfonyl)-1H-pyrrolo[2,3-b]pyridine (**32**) and 3-(3-(4-(1H-pyrrolo[2,3-b]pyridin-2-yl)-1H-1,2,3-triazol-1-yl)propyl)-1H-pyrrolo[2,3-b]pyridine (**33**)

The reaction mixture was cooled to room temperature and concentrated. The residue was purified by chromatography on silica gel column, CH_2Cl_2/MeOH 95:5, to give two fractions. Fraction 1: 146 mg of an orange solid which was triturated in EtOAc/CH_2Cl_2/cyclohexane, filtered, washed with water and diethyl ether, and dried to give 107 mg of the clean expected product **32** as a light brown solid in 47% yield. Fraction 2: 188 mg of a brown solid/oil which was triturated in EtOAc/CH_2Cl_2/cyclohexane, filtered, washed with water and diethylether, and dried to give 59 mg of the clean expected product **33** as a light brown solid in 37% yield.

4.3.14. 2-(1-(3-(1H-Pyrrolo[2,3-b]pyridin-3-yl)propyl)-1H-1,2,3-triazol-4-yl)-1-(phenylsulfonyl)-1H-pyrrolo[2,3-b]pyridine (**32**)

^{1}H NMR (300 MHz, DMSO-d_6) δ (ppm): 12.19 (br, 1H), 8.56 (s, 1H), 8.37 (dd, J = 1.5, 4.8 Hz, 1H), 8.26–8.15 (br, 1H), 8.12–8.05 (m, 3H), 7.95 (d, J = 7.8 Hz, 1H), 7.79 (s, 1H), 7.70 (dd, J = 7.5 Hz, 1H), 7.66–7.56 (m, 2H), 7.32 (dd, J = 4.8, 7.8 Hz, 1H), 7.07 (dd, J = 4.8, 7.8 Hz, 1H), 6.83 (s, 1H), 4.52 (t, J = 7.0 Hz, 2H), 2.79–2.70 (m, 2H), 2.35–2.22 (m, 2H). ^{13}C NMR (75 MHz, DMSO-d_6) δ (ppm): 147.4, 145.2 (2C), 143.2, 140.7, 138.1, 137.1, 135.1, 130.6, 130.0 (2C), 129.2, 128.3, 127.8 (2C), 123.8, 123.0, 122.2, 119.6, 119.0 (2C), 97.3, 49.6, 29.5, 21.7. HRMS-ESI (*m/z*): found 484.15571, calcd for $C_{25}H_{22}N_7O_2S$ $[M+H]^+$ 484.15502.

4.3.15. 3-(3-(4-(1H-Pyrrolo[2,3-b]pyridin-2-yl)-1H-1,2,3-triazol-1-yl)propyl)-1H-pyrrolo[2,3-b]pyridine (**33**)

^{1}H NMR (300 MHz, DMSO-d_6) δ (ppm): 12.18 (br, 1H), 11.41 (br, 1H), 8.55 (s, 1H), 8.23–8.17 (m, 2H), 7.97 (dd, J = 1.2, 3.5 Hz, 1H), 7.94 (dd, J = 1.2, 3.5 Hz, 1H), 7.33 (sd, J = 2.3 Hz, 1H), 7.07 (dd, J = 4.8, 7.9 Hz, 1H), 7.04 (dd, J = 4.8, 7.9 Hz, 1H), 6.83 (sd, J = 2.0 Hz, 1H), 4.50 (t, J = 7.0 Hz, 2H), 2.74 (t, J = 7.2 Hz, 2H), 2.26 (td, J = 7.0, 7.2 Hz, 2H). ^{13}C NMR (75 MHz, DMSO-d_6) δ (ppm): 149.5, 149.2, 143.2, 142.9, 140.6, 130.6, 128.3, 127.0, 123.6, 122.2, 121.0, 119.7, 116.5, 115.3, 112.4, 97.3, 49.8, 30.7, 22.1. HRMS-ESI (*m/z*): found 344.16199, calcd for $C_{19}H_{18}N_7$ $[M+H]^+$ 344.16182.

4.3.16. 3-(4-(1H-Pyrrolo[2,3-b]pyridin-2-yl)-1H-1,2,3-triazol-1-yl)-1-(1H-pyrrolo [2,3-b]pyridin-3-yl)propan-1-one (**34**)

The reaction mixture was cooled to room temperature and filtered. The filtrated was concentrated and triturated with cyclohexane/EtOAc. The two solids were gathered and washed with water and diethylether to give 78 mg of the expected product as a brown solid in 57% yield. ^{1}H NMR (300 MHz, DMSO-d_6) δ (ppm): 12.57 (br, 1H), 12.18 (br, 1H), 8.58 (d, J = 2.8 Hz, 1H), 8.55 (s, 1H), 8.48 (dd, J = 0.8, 7.8 Hz, 1H), 8.40–8.27 (br, 1H), 8.25–8.10 (br, 1H), 7.93 (d, J = 7.8 Hz, 1H), 7.26 (dd, J = 4.8, 7.8 Hz, 1H), 7.13–6.99 (m, 1H), 6.81 (s, 1H), 4.83 (t, J = 6.4 Hz, 2H), 3.65 (t, J = 6.4 Hz, 2H). ^{13}C NMR (75 MHz, DMSO-d_6) δ (ppm): 192.4, 149.4, 144.8, 140.4, 135.7, 135.3, 130.6, 130.0, 122.6, 118.9, 115.1, 97.3, 45.5, 38.8. HRMS-ESI (*m/z*): found 358.14135, calcd for $C_{19}H_{16}N_7O$ $[M+H]^+$ 358.14108.

4.3.17. 3-((4-(1H-Pyrrolo[2,3-b]pyridin-2-yl)-1H-1,2,3-triazol-1-yl)methyl)-1-(phenylsulfonyl)-1H-pyrrolo[2,3-b]pyridine (**35**)

The reaction mixture was cooled to room temperature and filtered. The solid was washed with MeOH and diethylether, and dried to give 72 mg of the expected product as a beige solid in 89% yield. ^{1}H NMR (300 MHz, DMSO-d_6) δ (ppm): 12.09 (br, 1H), 8.54 (s, 1H), 8.41 (dd, J = 1.2, 4.6 Hz, 1H), 8.23 (s, 1H), 8.21–8.11 (m, 3H), 8.03 (dd, J = 1.4, 7.9 Hz, 1H), 7.93 (d, J = 7.9 Hz, 1H), 7.74 (dd, J = 7.4 Hz, 1H), 7.64 (dd, J = 7.4, 7.8 Hz, 2H), 7.35 (dd, J = 4.8, 7.9 Hz, 1H), 7.05 (dd, J = 4.8, 7.9 Hz, 1H), 6.82 (sd, J = 1.8 Hz, 1H), 5.90 (s, 2H). ^{13}C NMR (75 MHz, DMSO-d_6) δ (ppm): 149.5, 147.1, 145.8, 143.3, 140.9, 137.8, 135.4, 130.3, 130.2 (2C), 129.4, 128.4, 128.1 (2C), 126.8, 122.1, 121.7, 120.9, 120.0, 116.5, 114.2, 97.5, 44.9. HRMS-ESI (*m/z*): found 456.12450, calcd for $C_{23}H_{18}N_7O_2S$ $[M+H]^+$ 456.12372.

4.3.18. 2-((4-(1H-Pyrrolo[2,3-b]pyridin-2-yl)-1H-1,2,3-triazol-1-yl)methyl)-1H-pyrrolo[2,3-b]pyridine (**36**)

The reaction mixture was cooled to room temperature and concentrated. The residue was purified by chromatography on silica gel column, CH_2Cl_2/MeOH 95:5, to give 97 mg of a light brown solid. The solid was triturated in MeOH and diethylether, filtered and dried. 64 mg of the expected product was obtained as a light brown solid in 53% yield. ^{1}H NMR (300 MHz, DMSO) δ (ppm): 12.14 (br, 1H), 11.98 (br, 1H), 8.51 (s, 1H), 8.30–8.12 (br, 2H), 8.00–7.90 (m, 2H), 7.13–7.02 (m, 2H), 6.85 (s, 1H), 6.55 (s, 1H), 5.85 (s, 2H). ^{13}C NMR (75 MHz, DMSO) δ (ppm): 149.4, 149.3, 143.6, 143.2, 140.7, 133.7, 130.4, 128.9, 128.3, 122.2 (2C), 116.8, 116.7, 116.5, 101.1, 97.4, 47.4. HRMS-ESI (*m/z*): found 316.13073, calcd for $C_{17}H_{14}N_7$ $[M+H]^+$ 316.13052.

4.4. Synthesis of compounds 38–44. General procedure for the ruthenium-catalyzed [3 + 2] cycloaddition reaction

4.4.1. 3-(2-(5-(1H-pyrrolo[2,3-b]pyridin-3-yl)-1H-1,2,3-triazol-1-yl)ethyl)-1H-pyrrolo[2,3-b]pyridine (**37**)

In a heat dried and nitrogen purged round bottom flask, **11a** (64 mg, 0.34 mmol), **4a** (61 mg, 0.43 mmol), Cp*RuCl(PPh_3)$_2$ (20 mg, 0.03 mmol) and THF (4 mL) were mixed and stirred under reflux for 60 h. The reaction mixture was cooled to room temperature, concentrated and purified by chromatography on silica gel column, CH_2Cl_2/MeOH 95:5–9:1, to give 46 mg of the expected product as an orange solid in 41% yield. ^{1}H NMR (300 MHz, DMSO) δ (ppm): 12.22 (br, 1H), 11.36 (br, 1H), 8.31 (dd, J = 1.5, 4.7 Hz, 1H), 8.12 (dd, J = 1.5, 4.7 Hz, 1H), 7.93 (s, 1H), 7.87 (dd, J = 1.2, 7.8 Hz, 1H), 7.68 (d, J = 2.7 Hz, 1H), 7.50 (dd, J = 1.2, 7.8 Hz, 1H), 7.11–7.15 (m, 2H), 6.89 (dd, J = 4.7, 7.8 Hz, 1H), 4.70 (t, J = 7.2 Hz, 2H), 3.20 (t, J = 7.2 Hz, 2H). ^{13}C NMR (75 MHz, DMSO) δ (ppm): 148.8, 148.7, 144.2, 142.9, 132.8, 131.6, 127.6, 126.4, 126.1, 124.2, 119.5, 118.3, 116.9, 115.3, 109.5, 100.0, 49.0, 25.9. HRMS-ESI (*m/z*): found 330.14622, calcd for $C_{18}H_{16}N_7$ $[M+H]^+$ 330.14617.

Compounds **38**–**44** were synthesized following the general procedure for the ruthenium-catalysed [3 + 2] cycloaddition reaction.

4.4.2. 2-(5-(1H-Pyrrolo[2,3-b]pyridin-3-yl)-1H-1,2,3-triazol-1-yl)-1-(1H-pyrrolo [2,3-b]pyridin-3-yl)ethan-1-one (**38**)

The reaction mixture was cooled to room temperature and filtered. The solid was washed with CH_2Cl_2, EtOAc and diethylether, and dried. 106 mg of the expected product was obtained as a brown

solid in 90% yield. ^{1}H NMR (300 MHz, DMSO) δ (ppm): 12.79 (br, 1H), 12.13 (br, 1H), 8.75 (sd, J = 2.0 Hz, 1H), 8.38 (dd, J = 1.5, 4.2 Hz, 1H), 8.36 (s, 1H), 8.31 (dd, J = 1.2, 4.6 Hz, 1H), 8.15 (s, 1H), 8.13 (d, J = 7.8 Hz, 1H), 7.69 (sd, J = 2.6 Hz, 1H), 7.26 (dd, J = 5.1, 7.5 Hz, 1H), 7.19 (dd, J = 4.7, 7.8 Hz, 1H), 6.12 (s, 2H). ^{13}C NMR (75 MHz, DMSO) δ (ppm): 187.4, 149.4, 148.7, 145.2, 144.3, 135.9, 132.8, 132.1, 129.9, 128.0, 125.4, 119.0, 118.2, 118.0, 117.0, 112.7, 100.2, 54.4. HRMS-ESI (*m/z*): found 344.12590, calcd for $C_{18}H_{15}N_7O$ $[M+H]^+$ 344.12543.

4.4.3. 3-(3-(5-(1H-Pyrrolo[2,3-b]pyridin-3-yl)-1H-1,2,3-triazol-1-yl)propyl)-1H-pyrrolo[2,3-b]pyridine (**39**)

The reaction mixture was cooled to room temperature and concentrated. The residu was purified by chromatography on silica gel column, CH_2Cl_2/MeOH 95:5–9:1, to give 80 mg of the expected product as an orange solid in 73% yield. ^{1}H NMR (300 MHz, DMSO) δ (ppm): 12.29 (br, 1H), 11.30 (br, 1H), 8.34 (dd, J = 1.5, 4.7 Hz, 1H), 8.14 (dd, J = 1.5, 4.7 Hz, 1H), 8.03 (dd, J = 1.5, 7.8 Hz, 1H), 8.01 (s, 1H), 7.91 (sd, J = 2.7 Hz, 1H), 7.72 (dd, J = 1.2, 7.8 Hz, 1H), 7.16 (dd, J = 4.7, 7.8 Hz, 1H), 7.16 (s, 1H), 6.93 (dd, J = 4.7, 7.8 Hz, 1H), 4.52 (t, J = 7.0 Hz, 2H), 2.63 (t, J = 7.4 Hz, 2H), 2.12 (td, J = 7.0, 7.4 Hz, 2H). ^{13}C NMR (75 MHz, DMSO) δ (ppm): 149.1, 148.8, 144.3, 142.8, 132.8, 131.5, 127.7, 126.7, 126.3, 123.3, 119.5, 118.3, 117.0, 115.2, 112.5, 100.0, 48.1, 30.1, 22.1. HRMS-ESI (*m/z*): found 344.16184, calcd for $C_{19}H_{18}N_7$ $[M+H]^+$ 344.16182.

4.4.4. 3-(5-(1H-Pyrrolo[2,3-b]pyridin-3-yl)-1H-1,2,3-triazol-1-yl)-1-(1H-pyrrolo [2,3-b]pyridin-3-yl)propan-1-one (**40**)

The reaction mixture was cooled to room temperature and concentrated. The residu was purified by chromatography on silica gel column, CH_2Cl_2/MeOH 95:5–9:1, to give 24 mg of the expected product as a yellow solid in 18% yield. ^{1}H NMR (300 MHz, DMSO) δ (ppm): 12.53 (br, 1H), 12.33 (br, 1H), 8.52 (s, 1H), 8.40 (dd, J = 1.4, 8.0 Hz, 1H), 8.34 (dd, J = 1.1, 4.6 Hz, 1H), 8.31 (dd, J = 1.2, 4.7 Hz, 1H), 8.08 (dd, J = 1.0, 7.8 Hz, 1H), 8.05 (sd, J = 2.5 Hz, 1H), 8.00 (s, 1H), 7.23 (dd, J = 4.8, 7.9 Hz, 1H), 7.19 (dd, J = 4.8, 8.0 Hz, 1H), 4.78 (t, J = 6.7 Hz, 2H), 3.64 (t, J = 6.7 Hz, 2H). ^{13}C NMR (75 MHz, DMSO) δ (ppm): 192.5, 149.4, 148.8, 144.7, 144.3, 135.2, 132.5, 131.8, 130.0, 127.8, 126.4, 118.6, 118.4, 118.0, 117.0, 115.1, 100.1, 44.0, 38.1. HRMS-ESI (*m/z*): found 358.14135, calcd for $C_{19}H_{16}N_7O$ $[M+H]^+$ 358.14108.

4.4.5. 3-(2-(5-(1H-Pyrrolo[2,3-b]pyridin-2-yl)-1H-1,2,3-triazol-1-yl)ethyl)-1H-pyrrolo[2,3-b]pyridine (**41**)

The reaction mixture was cooled to room temperature and concentrated. The residu was purified by chromatography on silica gel column, CH_2Cl_2/MeOH 95:5, to give 64 mg of the expected product as a brown solid in 62% yield. ^{1}H NMR (300 MHz, DMSO) δ (ppm): 12.30 (br, 1H), 11.41 (br, 1H), 8.31 (dd, J = 1.6, 4.7 Hz, 1H), 8.14 (dd, J = 1.6, 4.7 Hz, 1H), 8.13 (s, 1H), 8.00 (dd, J = 1.6, 7.9 Hz, 1H), 7.73 (dd, J = 1.2, 7.9 Hz, 1H), 7.21 (sd, J = 2.4 Hz, 1H), 7.14 (dd, J = 4.7, 7.9 Hz, 1H), 6.94 (dd, J = 4.6, 7.9 Hz, 1H), 6.77 (s, 1H), 4.89 (t, J = 7.2 Hz, 2H), 3.26 (t, J = 7.2 Hz, 2H). ^{13}C NMR (75 MHz, DMSO) δ (ppm): 149.5, 148.9, 144.7, 143.0, 133.5, 130.4, 129.2, 126.6, 124.7, 124.3, 120.6, 119.6, 116.9, 115.4, 109.2, 101.1, 49.8, 25.6. HRMS-ESI (*m/z*): found 330.14608, calcd for $C_{18}H_{16}N_7$ $[M+H]^+$ 330.14617.

4.4.6. 2-(5-(1H-Pyrrolo[2,3-b]pyridin-2-yl)-1H-1,2,3-triazol-1-yl)-1-(1H-pyrrolo [2,3-b]pyridin-3-yl)ethan-1-one (**42**)

The reaction mixture was cooled to room temperature and filtered. The solid was washed with CH_2Cl_2, EtOAc and diethylether, and dried. 113 mg of the expected product was obtained as a brown solid 97% yield. ^{1}H NMR (300 MHz, DMSO) δ (ppm): 12.83 (br, 1H), 12.37 (br, 1H), 8.84 (sd, J = 2.8 Hz, 1H), 8.37 (s, 1H), 8.35 (dd, J = 1.6, 4.7 Hz, 1H), 8.29 (s, 1H), 8.27 (dd, J = 1.6, 4.7 Hz, 1H), 7.91 (dd, J = 1.5, 7.9 Hz, 1H), 7.26 (dd, J = 5.0, 7.7 Hz, 1H), 7.05 (dd, J = 4.7, 7.9 Hz, 1H), 6.71 (sd, J = 2.0 Hz, 1H), 6.31 (s, 2H). ^{13}C NMR (75 MHz, DMSO) δ (ppm): 186.6, 149.4, 149.3, 145.2, 144.8, 136.0, 133.1, 131.8, 129.9, 129.3, 124.9, 120.5, 119.0, 118.0, 116.8, 112.5, 100.2, 55.3. HRMS-ESI (*m/z*): found 344.12580, calcd for $C_{18}H_{14}N_7O$ $[M+H]^+$ 344.12543.

4.4.7. 3-(3-(5-(1H-Pyrrolo[2,3-b]pyridin-2-yl)-1H-1,2,3-triazol-1-yl)propyl)-1H-pyrrolo[2,3-b]pyridine (**43**)

The reaction mixture was cooled to room temperature and concentrated. The residu was purified by chromatography on silica gel column, CH_2Cl_2/MeOH 95:5, to give 20 mg of the expected product as a brown solid in 18% yield. ^{1}H NMR (300 MHz, DMSO) δ (ppm): 12.30 (br, 1H), 11.41 (br, 1H), 8.29 (dd, J = 1.6, 4.7 Hz, 1H), 8.21–8.17 (m, 2H), 7.91–7.83 (m, 2H), 7.29 (sd, J = 2.4 Hz, 1H), 7.12 (dd, J = 4.7, 7.9 Hz, 1H), 6.98 (dd, J = 4.7, 7.9 Hz, 1H), 6.54 (dd, J = 2.0 Hz, 1H), 4.65 (t, J = 7.3 Hz, 2H), 2.78 (t, J = 7.3 Hz, 2H), 2.19 (td, J = 7.3 Hz, 2H). ^{13}C NMR (75 MHz, DMSO) δ (ppm): 149.4, 149.2, 144.8, 142.9, 133.3, 130.2, 129.17, 126.9, 124.7, 123.8, 120.5, 119.7, 116.8, 115.3, 112.3, 100.7, 48.7, 30.1, 22.0. HRMS-ESI (*m/z*): found 344.16226, calcd for $C_{19}H_{18}N_7$ $[M+H]^+$ 344.16182.

4.4.8. 3-(5-(1H-Pyrrolo[2,3-b]pyridin-2-yl)-1H-1,2,3-triazol-1-yl)-1-(1H-pyrrolo [2,3-b]pyridin-3-yl)propan-1-one (**44**)

The reaction mixture was cooled to room temperature and concentrated. The residu was purified by chromatography on silica gel column, CH_2Cl_2/MeOH 95:5, to give 52 mg of the expected product as a beige solid in 34% yield. ^{1}H NMR (300 MHz, DMSO) δ (ppm): 12.55 (br, 1H), 12.36 (br, 1H), 8.56 (s, 1H), 8.45 (d, J = 7.9 Hz, 1H), 8.36–8.30 (m, 2H), 8.17 (s, 1H), 8.06 (d, J = 7.9 Hz, 1H), 7.24 (dd, J = 4.8, 7.9 Hz, 1H), 7.15 (dd, J = 4.8, 7.9 Hz, 1H), 7.02 (s, 1H), 4.95 (t, J = 6.6 Hz, 2H), 3.70 (t, J = 6.6 Hz, 2H). ^{13}C NMR (75 MHz, DMSO) δ (ppm): 192.3, 149.5, 149.4, 144.8, 135.3, 133.3, 130.7, 130.0, 129.3, 124.8, 120.7, 118.6, 118.1, 117.9, 116.9, 115.0, 101.3, 44.8, 37.8. HRMS-ESI (*m/z*): found 358.14136, calcd for $C_{19}H_{16}N_7O$ $[M+H]^+$ 358.14108.

4.5. Cell maintenance and cytotoxicity assays

The cytotoxicity of the studied compounds was determined using cell lines of different histological origin as described earlier [46]. Briefly, compounds in three-fold dilutions were added to the cells in triplicate. The treatment lasted for 72 h, after which Calcein AM solution was added, and the fluorescence of live cells at 485 nm/538 nm (excitation/emission) was measured with a Fluoroskan Ascent microplate reader (Labsystems). IC_{50} (the drug concentration that reduced the number of viable cells to 50%) values were determined from the dose–response curves.

4.6. One-step cellular caspase-3/7 activity assay

The activity of cellular caspases-3/7 was measured according to published procedures [45]. Briefly, G361 cells were incubated in a density of 20,000 cells/well in a 96-well plate overnight. Next day, the compounds were added (the final concentration reached 2 μM) and the cells were incubated for the next 24 h. After incubation, 3x caspase-3/7 assay buffer (150 mM HEPES pH 7.4, 450 mM NaCl, 150 mM KCl, 30 mM $MgCl_2$, 1.2 mM EGTA, 1.5% Nonidet P40, 0.3% CHAPS, 30% sucrose, 30 mM DTT, 3 mM PMSF) with 37.5 μM Ac-DEVD-AMC as a substrate (Sigma–Aldrich) was added to the wells and plates were incubated at 37 °C. The caspase-3/7 activity was measured after 4 h using Fluoroskan Ascent microplate reader (Labsystems) at 346 nm/442 nm (excitation/emission).

4.7. Immunoblotting and antibodies

Immunoblotting analysis was performed as described earlier

[46]. Briefly, cellular lysates were prepared by harvesting cells in Laemmli sample buffer. Proteins were separated on SDS-polyacrylamide gels and electroblotted onto nitrocellulose membranes. After blocking, the membranes were incubated with specific primary antibodies overnight, washed and then incubated with peroxidase-conjugated secondary antibodies. Finally, peroxidase activity was detected with ECL + reagents (AP Biotech) using a CCD camera LAS-4000 (Fujifilm). Specific antibodies were purchased from Sigma–Aldrich (anti-α-tubulin, clone DM1A; peroxidase-labeled secondary antibodies), Santa Cruz Biotechnology (anti-cyclin B, clone GNS1; anti-Mcl-1, clone S-19; anti-PARP, clone F-2), Cell Signaling (anti-cyclin A, clone BF683; anti-Rb, clone 4H1; anti-pRb antibodies phosphorylated at S780 and S807/811; anti-pPP1α (T320); anti-PP1α; anti-pNPM (T199); anti-NPM; anti-caspase-7; anti-caspase-3, clone 3G2; anti-Bax, clone D2E11; anti-Bak, clone D4E4; anti-Bid), eBioscience (anti-5-bromo-2′-deoxyuridine-fluorescein, clone BU20A) or were a generous gift from prof. Bártek from Danish Cancer Society Research Center, Copenhagen, Denmark (anti-cyclin D1).

4.8. Kinase inhibition assays

CDK2/Cyclin E and CDK1/Cyclin B kinases were produced in Sf9 insect cells via baculoviral infection and purified on a Ni-NTA column (Qiagen). CDK4/Cyclin D1, CDK5/p35NCK, CDK7/Cyclin H/MAT1 and CDK9/Cyclin T1 were purchased from ProQinase GmbH. The kinases were assayed with 1 mg/mL histone H1 (for CDK1/2/5) or (YSPTSPS)2 KK peptide (for CDK7/CDK9) or RPPTLSPIPHIPR peptide (for CDK4) in the presence of 15/15/15/0.15/1.5/1.5 μM ATP (for CDK1/2/4/5/7/9), 0.05 μCi [γ-^{33}P]ATP and of the test compound in a final volume of 10 μL, all in a reaction buffer (60 mM HEPES-NaOH, pH 7.5, 3 mM $MgCl_2$, 3 mM $MnCl_2$, 3 μM Na-orthovanadate, 1.2 mM DTT, 2.5 μg/50 μl $PEG_{20.000}$). The reactions were stopped by adding 5 μL of 3% aq. H_3PO_4. Aliquots were spotted onto P-81 phosphocellulose (Whatman), washed 3 times with 0.5% aq. H_3PO_4 and finally air-dried. Kinase inhibition was quantified using a FLA-7000 digital image analyzer (Fujifilm). The concentration of the test compounds required to decrease the CDK activity by 50% was determined from dose–response curves and designated as IC_{50}.

4.9. Cell cycle analysis

The cultures were pulse-labeled with 10 μM 5-bromo-2′-deoxyuridine (BrdU) for 30 min at 37 °C prior to harvesting. The cells were then washed in PBS, fixed with 70% ethanol, and denatured in 2 M HCl. Following neutralization, the cells were stained with anti-BrdU fluorescein-labeled antibodies, washed, stained with propidium iodide and analyzed by flow cytometry using a 488 nm laser (Cell Lab Quanta SC, Beckman Coulter) as described previously [46].

4.10. Caspase activity assay

The cells were homogenized in an extraction buffer (10 mM KCl, 5 mM HEPES, 1 mM EDTA, 1 mM EGTA, 0.2% CHAPS, inhibitors of proteases, pH 7.4) on ice for 20 min. The homogenates were clarified by centrifugation at 10 000 × g for 30 min at 4 °C, and then the proteins were quantified and diluted to equal concentrations. Lysates were then incubated for 3 h with 100 μM Ac-DEVD-AMC as a substrate of caspases 3 and 7 in the assay buffer (25 mM PIPES, 2 mM EGTA, 2 mM $MgCl_2$, 5 mM DTT, pH 7.3). The fluorescence of the product was measured using a Fluoroskan Ascent microplate reader (Labsystems) at 355/460 nm (excitation/emission) as described previously [46].

4.11. Molecular docking study

3D structures of compounds were prepared with Marvin, a software used for drawing, displaying, and characterizing chemical structures, substructures, and reactions [Marvin 14.7.7, 2014, ChemAxon (http://www.chemaxon.com)]. 3D structures of ligands were optimized and all hydrogens were added within the MarvinSketch 14.7.7 program. All nonaromatic and nonring bonds were set as rotatable within AutoDock Tools 1.5.4 program [47]. The crystal structure for CDK2 with roscovitin (PDBID: 2A4L) was used as the protein docking template with a docking grid of 16 Å around the center of the ligand in the crystal structure, which was deleted prior to docking. Polar hydrogens were added to receptor or selected for all ligands with the AutoDock Tools program prior to docking with the Autodock Vina 1.1.2 program [48].

Author contributions

The manuscript was written through contributions of all authors. All authors have given approval to the final version of the manuscript.

Acknowledgments

This work was supported by the European funds for the economical and regional development (FEDER), the Laboratory of excellence Labex SYNORG, ANR-11-LABX-0029 and the Medical Research Fondation (FRM: SPF20130526815). The authors also gratefully acknowledge support through the projects LO1305 and LO1204 from the Ministry of Education, Youth and Sports of the Czech Republic. The work was also supported by the Czech Science Foundation (grant 15-17282Y) and by student projects IGA_PrF_2015_027 and IGA_PrF_2015_024 of Palacky University in Olomouc.

Appendix A. Supplementary data

Supplementary data related to this article can be found at http://dx.doi.org/10.1016/j.ejmech.2015.12.023.

References

[1] M. Malumbres, M. Barbacid, Mammalian cyclin-dependent kinases, Trends Biochem. Sci. 30 (2005) 630–641.
[2] A.M. Senderowicz, Small molecule modulators of cyclin-dependent kinases for cancer therapy, Oncogene 19 (2000) 6600–6606.
[3] S. Lim, P. Kaldis, Cdks, cyclins and CKIs: roles beyond cell cycle regulation, Development 140 (2013) 3079–3093.
[4] A. Deshpande, P. Sicinski, P.W. Hinds, Cyclins and Cdks in development and cancer: a perspective, Oncogene 24 (2005) 2909–2915.
[5] J.S. Blachly, J.C. Byrd, Emerging drug profile: cyclin-dependent kinase inhibitors, Leukemia Lymphoma 54 (2013) 2133–2143.
[6] U. Asghar, A.K. Witkiewicz, N.C. Turner, E.S. Knudsen, The history and future of targeting cyclin-dependent kinases in cancer therapy, Nat. Rev. Drug Discov. 14 (2015) 130–146.
[7] N. Kwiatkowski, T. Zhang, P.B. Rahl, B.J. Abraham, J. Reddy, S.B. Ficarro, A. Dastur, A. Amzallag, S. Ramaswamy, B. Tesar, C.E. Jenkins, N.M. Hannett, D. McMillin, T. Sanda, T. Sim, N.D. Kim, T. Look, C.S. Mitsiades, A.P. Weng, J.R. Brown, C.H. Benes, J.A. Marto, R.A. Young, N.S. Gray, Targeting transcription regulation in cancer with a covalent CDK7 inhibitor, Nature 511 (2014) 616–620.
[8] D.W. Fry, P.J. Harvey, P.R. Keller, W.L. Elliott, M. Meade, E. Trachet, M. Albassam, X. Zheng, W.R. Leopold, N.K. Pryer, P.L. Toogood, Specific inhibition of cyclin-dependent kinase 4/6 by PD 0332991 and associated antitumor activity in human tumor xenografts, Mol. Cancer Ther. 3 (2004) 1427–1438.
[9] D. Cai, V.M. Latham Jr., X. Zhang, G.I. Shapiro, Combined depletion of cell cycle and transcriptional cyclin-dependent kinase activities induces apoptosis in cancer cells, Cancer Res. 66 (2006) 9270–9280.
[10] A. Echalier, E. Cot, A. Camasses, E. Hodimont, F. Hoh, P. Jay, F. Sheinerman, L. Krasinska, D. Fisher, An integrated chemical biology approach provides insight into Cdk2 functional redundancy and inhibitor sensitivity, Chem. Biol.

19 (2012) 1028–1040.
[11] R. Soni, L. Muller, P. Furet, J. Schoepfer, C. Stephan, S. Zumstein-Mecker, H. Fretz, B. Chaudhuri, Inhibition of cyclin-dependent kinase 4 (Cdk4) by fascaplysin, a marine natural product, Biochem. Biophys. Res. Commun. 275 (2000) 877–884.
[12] P.R. Jenkins, J. Wilson, D. Emmerson, M.D. Garcia, M.R. Smith, S.J. Gray, R.G. Britton, S. Mahale, B. Chaudhuri, Design, synthesis and biological evaluation of new tryptamine and tetrahydro-β-carboline-based selective inhibitors of CDK4, Bioorg. Med. Chem. 16 (2008) 7728–7739.
[13] C. Aubry, A.J. Wilson, D. Emmerson, E. Murphy, Y.Y. Chan, M.P. Dickens, M.D. García, P.R. Jenkins, S. Mahale, B. Chaudhuri, Fascaplysin-inspired diindolyls as selective inhibitors of CDK4/cyclin D1, Bioorg. Med. Chem. 17 (2009) 6073–6084.
[14] S. Mahale, C. Aubry, A.J. Wilson, P.R. Jenkins, J.-D. Maréchal, M.J. Sutcliffe, B. Chaudhuri, CA224, a non-planar analogue of fascaplysin, inhibits Cdk4 but not Cdk2 and arrests cells at G0/G1 inhibiting pRB phosphorylation, Bioorg. Med. Chem. Lett. 16 (2006) 4272–4278.
[15] A. Hörmann, B. Chaudhuri, H. Fretz, DNA binding properties of the marine sponge pigment fascaplysin, Bioorg. Med. Chem. 9 (2001) 917–921.
[16] CDK4/cyclin D inhibitory activities of 21 and 22 were performed by the Cerep company. The results are presented in the supporting informations.
[17] R. Huisgen, 1,3-Dipolar cycloadditions. Past and future, Angew. Chem. Int. Ed. 2 (1963) 565–632.
[18] K. Sonogashira, Y. Tohda, N. Hagihara, A convenient synthesis of acetylenes: catalytic substitutions of acetylenic hydrogen with bromoalkenes, iodoarenes and bromopyridines, Tetrahedron Lett. 16 (1975) 4467–4470.
[19] S. Thorand, N. Krause, Improved procedures for the palladium-catalyzed coupling of terminal Alkynes with aryl bromides (sonogashira coupling), J. Org. Chem. 63 (1998) 8551–8553.
[20] R. Chinchilla, C. Nájera, The sonogashira reaction: a booming methodology in synthetic organic chemistry, Chem. Rev. 107 (2007) 874–922.
[21] C. Chaulet, C. Croix, D. Alagille, S. Normand, A. Delwail, L. Favot, J.-C. Lecron, M.-C. Viaud-Massuard, Design, synthesis and biological evaluation of new thalidomide analogues as TNF-α and IL-6 production Inhibitors, Bioorg. Med. Chem. Lett. 21 (2011) 1019–1022.
[22] H. Naka, Y. Akagi, K. Yamada, T. Imahori, T. Kasahara, Y. Kondo, Fluorous synthesis of yuehchukene by α-lithiation of perfluoroalkyl-tagged 1-(arylsulfonyl)indole with mesityllithium, Eur. J. Org. Chem. (2007) 4635–4637.
[23] T. Greene, P.G.M. Wuts, Protective Groups in Organic Synthesis, third ed., John Wiley & Sons, New York, 1991.
[24] C. Galvez, P. Viladoms, Reactivity of 1H-pyrrolo[2,3-b]pyridine. II. Synthesis of 3-(β-haloethyl)-7-azaindole, J. Heterocycl. Chem. 21 (1984) 421–425.
[25] J. Blum, D. Gelman, W. Baidossi, E. Shakh, A. Rosenfeld, Z. Aizenshtat, Palladium-catalyzed methylation of Aryl and vinyl halides by stabilized methylaluminum and methylgallium complexes, J. Org. Chem. 62 (1997) 8681–8686.
[26] N. Joubert, R. Pohl, B. Klepetářová, M. Hocek, Modular and practical synthesis of 6-substituted pyridin-3-yl C-nucleosides, J. Org. Chem. 72 (2007) 6797–6805.
[27] R. Liu, P. Zhang, T. Gan, J.M. Cook, Regiospecific bromination of 3-methylindoles with NBS and its application to the concise synthesis of optically active unusual tryptophans present in marine cyclic peptides[1], J. Org. Chem. 62 (1997) 7447–7456.
[28] V. D'Elia, L. Yinghao, H. Zipse, Immobilized DMAP derivatives rivaling homogeneous DMAP, Eur. J. Org. Chem. (2011) 1527–1533.
[29] V. Aucagne, D.A. Leigh, Chemoselective formation of successive triazole linkages in one pot: "click–click" chemistry, Org. Lett. 8 (2006) 4505–4507.
[30] Regarding entries 11 and 13, it should be noted that even if compounds 30 and 33 could have been obtained directly by cycloaddition between the azide derivatives 11a or 11b and the alkyne derivative 4b, we did not attempt these reactions since 30 and 33 were obtained in a good yield for two steps and in enough quantity for their characterization and biological evaluation.
[31] L. Zhang, X. Chen, P. Xue, H.H.Y. Sun, I.D. Williams, K.B. Sharpless, V.V. Fokin, G. Jia, Ruthenium-catalyzed cycloaddition of alkynes and organic azides, J. Am. Chem. Soc. 127 (2005) 15998–15999.
[32] R.D. Cramer, D.E. Patterson, J.D. Bunce, Comparative molecular field analysis (CoMFA). 1. effect of shape on binding of steroids to carrier proteins, J. Am. Chem. Soc. 110 (1988) 5959–5967.
[33] G. Klebe, U.J. Abraham, Comparative molecular similarity index analysis (CoMSIA) to study hydrogen-bonding properties and to score combinatorial libraries, J. Comput. Aided Mol. Des. 13 (1999) 1–10.
[34] The references for the molecules used in the training and the test sets can be found in the supplementary data.
[35] TRIPOS, 1699 South Hanley Road, St. Louis, MO 63144, USA.
[36] M.C. Clark, R.D. Cramer III, N. van Opden Bosch, Validation of the general purpose tripos 5.2 force field, J. Comput. Chem. 10 (1989) 982–1012.
[37] S.J. Cho, A. Tropsha, Cross-validated R2-guided region selection for comparative molecular field analysis: a simple method to achieve consistent results, J. Med. Chem. 38 (1995) 1060–1066.
[38] B. Kramer, M. Rarey, T. Lengauer, Evaluation of the FLEXX incremental construction algorithm for protein–ligand docking, Proteins Struct. Funct. Genet. 37 (1999) 228–241.
[39] J. Gasteiger, M. Marsili, Iterative partial equalization of orbital electronegativity—a rapid access to atomic charges, Tetrahedron 36 (1980) 3219–3288.
[40] B.L. Bush, R.B. Nachbar Jr., Sample-distance partial least squares: PLS optimized for many variables, with application to CoMFA, J. Comput. Aided Mol. Des. 7 (1993) 587–619.
[41] A.R. Leach, Molecular Modelling: Principles and Applications, Henry Ling, London, 2001, p. 695.
[42] T. Gucky, R. Jorda, M. Zatloukal, V. Bazgier, K. Berka, E. Reznickova, T. Beres, M. Strnad, V. Krystof, A novel series of highly potent 2,6,9-trisubstituted purine cyclin-dependent kinase inhibitors, J. Med. Chem. 56 (2013) 6234–6247.
[43] M. Payton, G. Chung, P. Yakowec, A. Wong, D. Powers, L. Xiong, N. Zhang, J. Leal, T.L. Bush, V. Santora, B. Askew, A. Tasker, R. Radinsky, R. Kendall, S. Coats, Discovery and evaluation of dual CDK1 and CDK2 inhibitors, Cancer Res. 66 (2006) 4299–4308.
[44] M. Zatloukal, R. Jorda, T. Gucky, E. Reznickova, J. Voller, T. Pospisil, V. Malinkova, H. Adamcova, V. Krystof, M. Strnad, Synthes in vitro biological evaluation of 2,6,9-trisubstituted purines targeting multiple cyclin-dependent kinases, Eur. J. Med. Chem. 61 (2013) 61–72.
[45] R.A. Carrasco, N.B. Stamm, B.K.R. Patel, One-step cellular caspase-3/7 assay, Biotechniques 34 (2003) 1064–1067.
[46] V. Krystof, I.W. McNae, M.D. Walkinshaw, P.M. Fischer, P. Muller, B. Vojtesek, M. Orsag, L. Havlicek, M. Strnad, Antiproliferative activity of olomoucine II, a novel 2,6,9-trisubstituted purine cyclin-dependent kinase inhibitor, Cell Mol. Life Sci. 62 (2005) 1763–1771.
[47] M.F. Sanner, Python: a programming language for software integration and development, J. Mol. Graph. Model. 17 (1999) 57–61.
[48] O. Trott, A.J. Olson, Autodock vina: improving the speed and accuracy of docking with a new scoring function, efficient optimization, and multithreading, J. Comput. Chem. 31 (2010) 455–461.